Supporting Information

Synthesis, crystal growth, structure and photophysical properties of decafluoroanthracene and its co-crystals with polycyclic arenes

Alexandra Friedrich,[a]* Lisa Schraut-May,[b] Florian Rauch,[a] Pablo Durand,[c] Johannes Krebs,[a] Paul N. Ruth,[d] Sebastian Hammer,[b] Rüdiger Bertermann,[a] Maik Finze,[a] Stewart J. Clark,[e]* Jens Pflaum,[b,f]* Nicolas Leclerc,[c]* and Todd B. Marder [a]*

[a] Julius-Maximilians-Universität Würzburg, Institut für Anorganische Chemie, Am Hubland, 97074 Würzburg, Germany. E-mails: alexandra.friedrich1@uni-wuerzburg.de; todd.marder@uni-wuerzburg.de

[b] Julius-Maximilian University Würzburg, Experimental Physics VI, Am Hubland, 97074 Würzburg, Germany. E-mail: jens.pflaum@uni-wuerzburg.de

[c] Université de Strasbourg-CNRS, ICPEES – UMR7515, 67087 Strasbourg, France. E-mail: leclercn@unistra.fr

[d] University of Durham, Advanced Research Computing, The Lodge, Lower Mountjoy, South Road, DH1 3LE, UK

[e] University of Durham, Department of Physics, Science Labs, South Road, Durham DH1 3LE, UK. E-mail: s.j.clark@durham.ac.uk

[f] Center for Applied Energy Research (CAE Bayern e.V.), 97074 Würzburg, Germany

Table of Contents

I. General experimental and computational details

Synthesis and characterization. Naphthalene, anthracene, pyrene, perylene, triphenylene, and reagents for the synthesis of decafluoroanthracene (**DFA**) were purchased from commercial suppliers and used without further purifications. When possible, compound purifications were performed on standard silica gel (0.063-0.200 mm). Silica plates precoated with fluorescent indicator were used to perform thin layer chromatography. Tetracene was purchased from Sigma Aldrich and was purified twice by gradient sublimation prior to use.

Crystal growth. All co-crystals were grown under an argon atmosphere inside a glovebox. The individual components were dissolved in a 1:1 stoichiometric ratio in dichloromethane. Co-crystals of **DFA** with naphthalene (**NDFA**), anthracene (**ADFA**), tetracene (**TetDFA**), pyrene (**PyrDFA**), perylene (**PerDFA**) and triphenylene (**TriDFA**), as well as crystals of the tetracene-**DFA** dimer (**TetDFA-Dimer**), were obtained by slow solvent evaporation into grease of saturated dichloromethane solutions. Grease was used as a 'sponge' to absorb the solvent in a closed system in order to protect the catalyst of the glovebox. In the case of orange coloured **TetDFA** co-crystals, all steps were performed in the absence of light to avoid dimerization. For the dedicated growth of the colourless **TetDFA-Dimer** single crystals, the solution was stirred at room temperature and irradiated with a 375 nm UV lamp until the yellow solution turned colourless.

NMR spectroscopy. ^{19}F NMR spectra of compounds **1**, **2**, **3** and **4** were recorded on a Bruker Avance 400 NMR spectrometer (operating at ^{19}F: 376.7 MHz) at 298 K. NMR spectra of **DFA** and **TetDFA-Dimer** were recorded on a Bruker Avance Neo I 600 NMR spectrometer (operating at ^{1}H: 600.2 MHz, ^{19}F: 564.8 MHz, ^{13}C: 150.9 MHz) and on a Bruker Avance Neo I 500 NMR spectrometer (operating at ^{1}H: 500.1 MHz, ^{19}F: 470.6 MHz, ^{13}C: 125.8 MHz) at 298 K. ^{1}H and ^{13}C ($\Xi(^{13}C)$ = 25.145020 MHz) chemical shifts were calibrated against the residual solvent signal and the solvent signal, respectively ($\delta(^{1}H)$: $CHDCl_2$ 5.32 ppm; $\delta(^{13}C)$: CD_2Cl_2 53.5 ppm. The ^{19}F NMR signals were referenced against $CFCl_3$ with $\Xi(^{19}F)$ = 94.094011 MHz. Chemical shifts (δ) are reported in ppm.

High resolution mass spectroscopy. HRMS were recorded using a Thermo Scientific Exactive Plus Orbitrap MS system with either an Atmospheric Sample Analysis Probe (ASAP) or by Electrospray Ionization (ESI).

Photophysical measurements.

Excitation and emission spectra of **NDFA**, **TriDFA**, **TetDFA**, **PyrDFA** and **ADFA**, were recorded using an Edinburgh Instruments FLSP920 spectrometer equipped with a double monochromator for both excitation and emission, operating in right-angle geometry mode, and all spectra were fully corrected for the spectral response of the instrument. The crystals were inserted into standard quartz cuvettes (1 cm × 1 cm cross-section). Measurements on **PerDFA** were not feasible with this method, as it formed very thin, small crystals which had some additional perylene attached to them, which distorted the spectra. **Polarisation dependent photoluminescence spectra** of **ADFA**, **TetDFA** and **PerDFA** were conducted with a micro-photoluminescence setup illuminating single co-crystals with a 405 nm circular polarised cw-laser. The emission spectra were recorded polarisation dependent with a Princeton Instruments Acton SP-2500i spectrometer with a PIXIS 100BR_eXcelon CCD camera and additional polarisation filters. **Luminescence lifetimes** were recorded using the time-correlated single-photon counting (TCSPC) method using the same FLSP920 spectrometer described above with a picosecond pulsed diode laser at emission maxima of 376.6 nm or 472 nm for **TetDFA**. The full width at half maximum (FWHM) of the laser pulses were 72.6 ps (at 376.6 nm) or 91 ps (at 472 nm), respectively, while the instrument response function (IRF) had a FWHM of ca. 1.0 ns, measured from the scatter of $BaSO_4$ at the excitation wavelength. Decays were recorded to at least 10000 counts in the peak channel with a record length of at least 1000 channels. The band pass of the monochromator was adjusted to give a signal count rate of <10 kHz. Iterative reconvolution of the IRF with one decay function and non-linear least-squares analysis were used to analyze the data. The quality of the fit was judged by the calculated value of the reduced χ^2 and visual inspection of the weighted residuals.

Crystal structure analysis.

Crystal structure determination at ambient and low temperature. Crystals suitable for single-crystal X-ray diffraction were selected, coated in perfluoropolyether oil, and mounted on polyimide microloops. Diffraction data were collected on a Rigaku Oxford Diffraction XtaLAB Synergy diffractometer with a semiconductor HPA-detector (HyPix-Arc-150 or HyPix-6000 (**ADFA** at 100 K)) and multi-layer mirror monochromated Cu-K_α radiation generated by a PhotonJet-R or a PhotonJet (**ADFA** at 100 K) source. The temperature was regulated using an Oxford Cryostream low-temperature device. Diffraction data were collected at 100 K (all compounds), 200 K (**ADFA**), and ambient temperature (**NDFA**, **ADFA**, **TetDFA**, **TetDFA-Dimer**, **PyrDFA**, and **TriDFA**). The images were processed and corrected for

Lorentz-polarisation effects and absorption (empirical scaling) using the CrysAlis^{Pro} software from Rigaku Oxford Diffraction. The structures were solved using the intrinsic phasing method (SHELXT)[1] and Fourier expansion technique. All non-hydrogen atoms were refined in anisotropic approximation, with hydrogen atoms 'riding' in idealized positions, by full-matrix least squares against F^2 of all data, using SHELXL[2] software and the SHELXLE[3] graphical user interface. The crystal structure of **NDFA** at 100 K was refined as a two-component twin with component two rotated by -179.98° around [0.96 0.00 -0.27] (reciprocal) or [1.00 0.00 -0.00] (direct) axis. The twin fraction was refined to 19%. Diamond[4] software was used for graphical representation. Other structural information was extracted using OLEX2[5] software. Crystal data and experimental details at 100 K and at 200 K or ambient temperature are listed in Tables S2 and S3, respectively; full structural information has been deposited with the Cambridge Crystallographic Data Centre. CCDC-2293625 (**DFA**), 2293626 – 2293627 (**NDFA**), 2293628 – 2293630 (**ADFA**), 2293631 – 2293632 (**TetDFA**), 2293633 – 2293634 (**TetDFA_Dimer**), 2293635 – 2293636 (**PyrDFA**), 2293637 (**PerDFA**), and 2293638 – 2293639 (**TriDFA**).

Hirshfeld surface analysis. In order to compare and classify the types and magnitudes of the intermolecular interactions within the co-crystals, the concept of Hirshfeld surface analysis was applied.[6-9] Hirshfeld surfaces were calculated and analysed using the CrystalExplorer[10] program. The volume of the surface of the crystal's voids was obtained from the Hirshfeld analysis.[11] In order to quantify the nature and type of intermolecular interactions from the Hirshfeld surface analysis in a two-dimensional, graphical way, fingerprint plots and their breakdown to the individual contributions were used.[12-14]

Computational details. Density functional calculations using the PBE[15] exchange-correlation functional within the CASTEP code[16] were used to calculate the relaxed geometry for the set of molecules. A plane wave basis set is used which requires periodic boundary conditions, therefore each molecule was placed in a large supercell to isolate it from periodic images. The resultant electrostatic potential (on a regular numerical grid) was obtained and we took a 2D slice through the plane of the molecule and plotted contours.

II. Synthesis and characterization

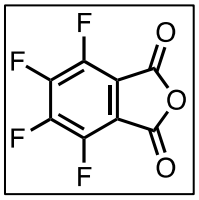

Tetrafluorophthalic anhydride (1): To a 100 mL round bottom flask was added tetrafluorophthalic acid (5 g, 2.1 mmol) and thionyl chloride (6.5 mL, 3.4 mmol). The reaction was refluxed overnight and then thionyl chloride was removed under vacuum leaving a brown solid which was sublimed under vacuum to give 4.1 g of a white solid. Yield = 90 %.

^{19}F NMR (acetone-d_6, 376.7 MHz) δ (ppm): -140.1 (m, 4F); -153.07 (m, 4F).

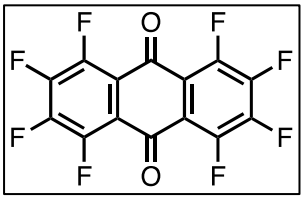

1,2,3,4,5,6,7,8-octafluoroanthracene-9,10-dione (2): To a dried 100 mL round bottom flask equipped with an addition funnel and distillation apparatus was added dry CsF (5 g, 33 mmol), *m*-xylene (50 mL) and tetrafluorophthalic anhydride (**1**) (5 g, 23 mmol). The mixture was refluxed for 30 min and then dry sulfolane (30 mL) was added dropwise. The reaction was followed by monitoring the amount of gas (CO_2) evolved and was stopped when gas evolution ceased (ca. 45 min). The xylene was removed by vacuum distillation. The remaining red liquid was diluted with 50 mL of water and the orange precipitate was collected by filtration and washed with a 1:1 MeOH/water solution. The resulting yellow powder was then recrystallized from toluene to give 1.5 g of pale-yellow needles. Yield = 40 %.

^{19}F NMR ($CDCl_3$, 376.7MHz) δ (ppm): -137.4 (m, 4F); -143.3 (m, 4F).

^{19}F NMR literature values (ppm) by Tannaci *et al.* (2007) are: -137.39 (m, 4F), -143.34 (m, 4F).[17]

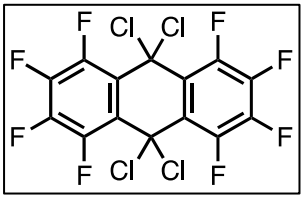

9,9,10,10-tetrachloro-1,2,3,4,5,6,7,8-octafluoro-9,10-dihydroanthracene (3): To a 100 mL Schlenk flask was added 1,2,3,4,5,6,7,8-octafluoroanthracene-9,10-dione (**2**) (2.8 g, 7.9 mmol), PCl_5 (5.96 g, 0.29 mmol) and diphenylphosphonic dichloride (15.5 g, 7.9 mmol). The reaction was kept at 170 °C for 24 h, then the mixture was diluted in toluene, washed with water until the organic layer appeared clear, and washed with $NaHCO_3$ solution. The solvent was evaporated and the solid was washed with MeOH to give 2.5 g of a yellow powder. Yield = 70 %.

^{19}F NMR ($CDCl_3$, 376.7MHz) δ (ppm): -128.61 (m, 4F), -150.11 (m, 4F).

^{19}F NMR literature values (ppm) by Tannaci *et al.* (2007) are: -128.61 (m, 4F), -150.11 (m, 4F).[17]

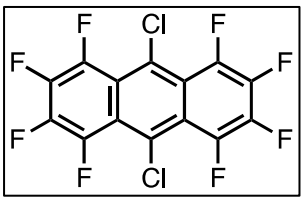

9,10-dichloro-1,2,3,4,5,6,7,8-octafluoroanthracene (4): To a 500 mL flask was added 9,9,10,10-tetrachloro-1,2,3,4,5,6,7,8-octafluoro-9,10-dihydroanthracene (**3**) (8.5 g, 18.4 mmol), NMP (150 mL) and AcOH (50 mL). The flask was heated under argon for 24 h. The mixture was extracted with toluene, washed with aqueous $NaHCO_3$ and then brine. The solvent was evaporated leaving a black oil which was treated with MeOH to precipitate a white powder. The product was diluted in chloroform and filtered onto silica gel, the cake was washed with petroleum ether, and the solvent evaporated to give 6 g of a white powder. Yield = 80 %.

^{19}F NMR ($CDCl_3$, 376.7MHz) δ (ppm): -137.1 (m, 4F), -152.4 (m, 4F).

^{19}F NMR literature values (ppm) by Tannaci *et al.* (2007) are: -137.09 (d, 4F, J = 12 Hz), -152.35 (d, 4F, J = 12 Hz).[17]

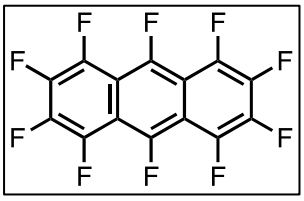

Decafluoroanthracene (DFA): To a 100 mL round bottom flask equipped with a distillation apparatus and addition funnel was added sulfolane (20 mL) and KF (0.5 g, 8.7 mmol). The funnel was charged with 9,10-dichloro-1,2,3,4,5,6,7,8-octafluoroanthracene (**4**) (0.85 g, 2.17 mmol), 18-crown-6 (115 mg, 0.43 mmol), and toluene (50 mL). The flask was heated to 200°C while the solution of **4** was added at a rate of 1 drop per second. Toluene distilled out of the flask and, at the end of the addition, the reaction was monitored by TLC. When reaction was complete, the mixture was diluted in toluene, washed with water, and filtered onto silica gel. The product was then purified by column chromatography using petroleum ether as the eluent. The solvent was removed under vacuum to give 0.6 g of a yellow powder. Yield = 80 %.

^{19}F NMR ($CDCl_3$, 470.6 MHz) δ (ppm): -122.1 (m, 2F, J_{TS} = 74.2 Hz), -144.3 (m, 4F, J_{TS} = 74.2 Hz), -152.3 (m, 4F). J_{TS} represents the F,F through-space coupling constant for direct spin,spin-interactions between fluorine atoms across the space.

TetDFA-Dimer:

$^{1}H\{^{19}F\}$ NMR (CD_2Cl_2, 600.2 MHz) δ (ppm): 7.74 (m, 2H), 7.72 (s, 2H), 7.46 (m, 2H), 7.29 (m, 2H), 7.11 (m, 2H), 5.04 (s, 2H).

^{1}H NMR (CD_2Cl_2, 600.2 MHz) δ (ppm): 7.74 (m, 2H), 7.72 (s, 2H), 7.46 (m, 2H), 7.29 (m, 2H), 7.11 (m, 2H), 5.04 (d, $J_{F,H}$ = 31.8 Hz, 2H).

^{19}F NMR (CD_2Cl_2, 564.8 MHz) δ (ppm): -143.1 (m, 4F), -152.8 (m, 2F), -154.5 (m, 4F).

$^{19}F\{^{1}H\}$ NMR (CD_2Cl_2, 564.8 MHz) δ (ppm): -143.1 (m, 4F), -152.8 (m, 2F), -154.5 (m, 4F).

$^{13}C\{^{1}H\}$ NMR (CD_2Cl_2, 125.8 MHz) δ (ppm): 139.6 (d, J = 3.6 Hz), 136.4 (d, J = 3.6 Hz), 132.4, 128.3, 127.7, 127.3, 126.9, 126.3, 101.8 (d, J = 210.5 Hz), 62.6 (d, J = 33.6 Hz).

$^{13}C\{^{19}F\}$: (CD_2Cl_2, 125.8 MHz) δ (ppm): 143.2, 143.2, 140.3, 140.2, 120.4, 101.8 (d, J = 7.9 Hz).

$^{13}C\{^{1}H,^{19}F\}$: (CD_2Cl_2, 150.9 MHz) δ (ppm): 143.2, 143.1, 140.2, 140.1, 139.6, 136.3, 132.4, 128.3, 127.7, 127.3, 126.9, 126.3, 120.4, 101.8, 62.5.

III. NMR spectra

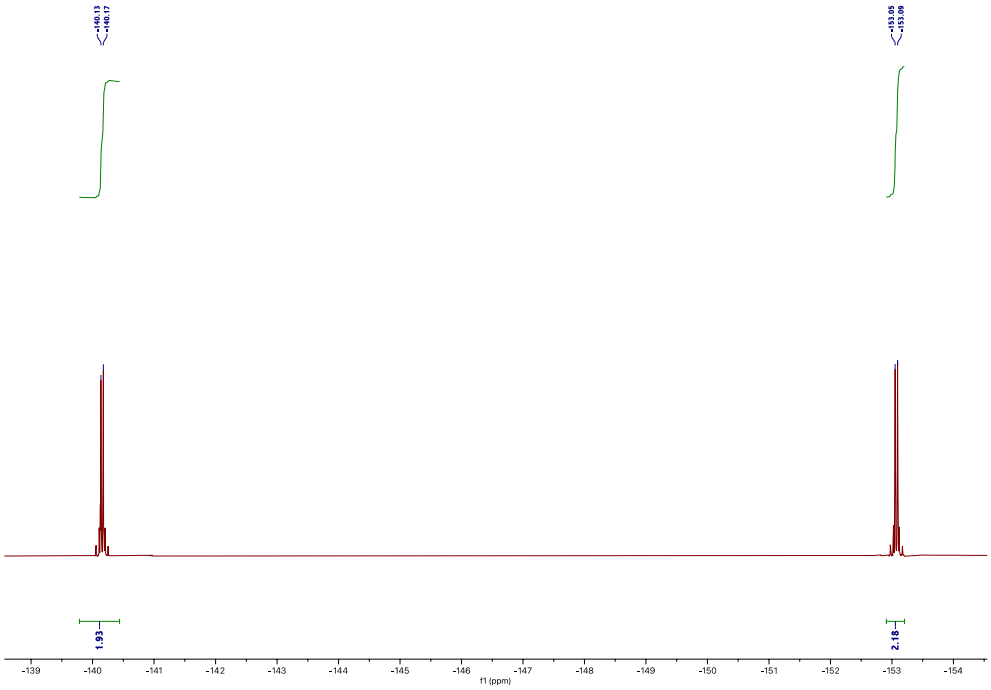

Figure S1. ^{19}F NMR spectrum of **1** in $CDCl_3$ (376.7 MHz).

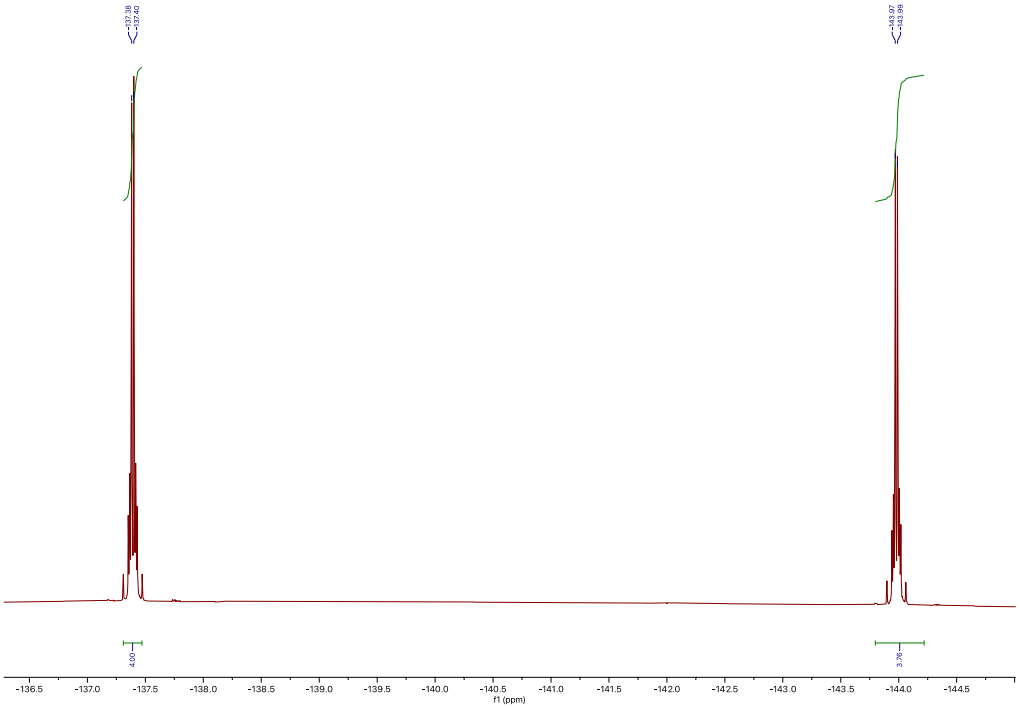

Figure S2. ^{19}F NMR spectrum of **2** in $CDCl_3$ (376.7 MHz).

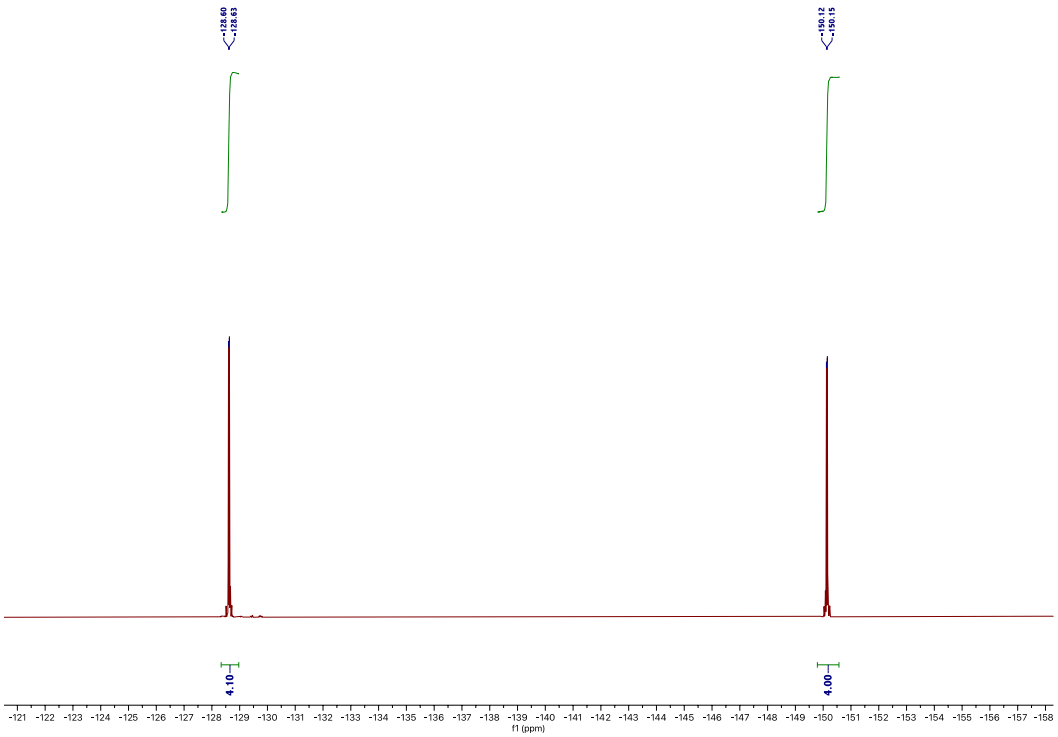

Figure S3. ^{19}F NMR spectrum of **3** in $CDCl_3$ (376.7 MHz).

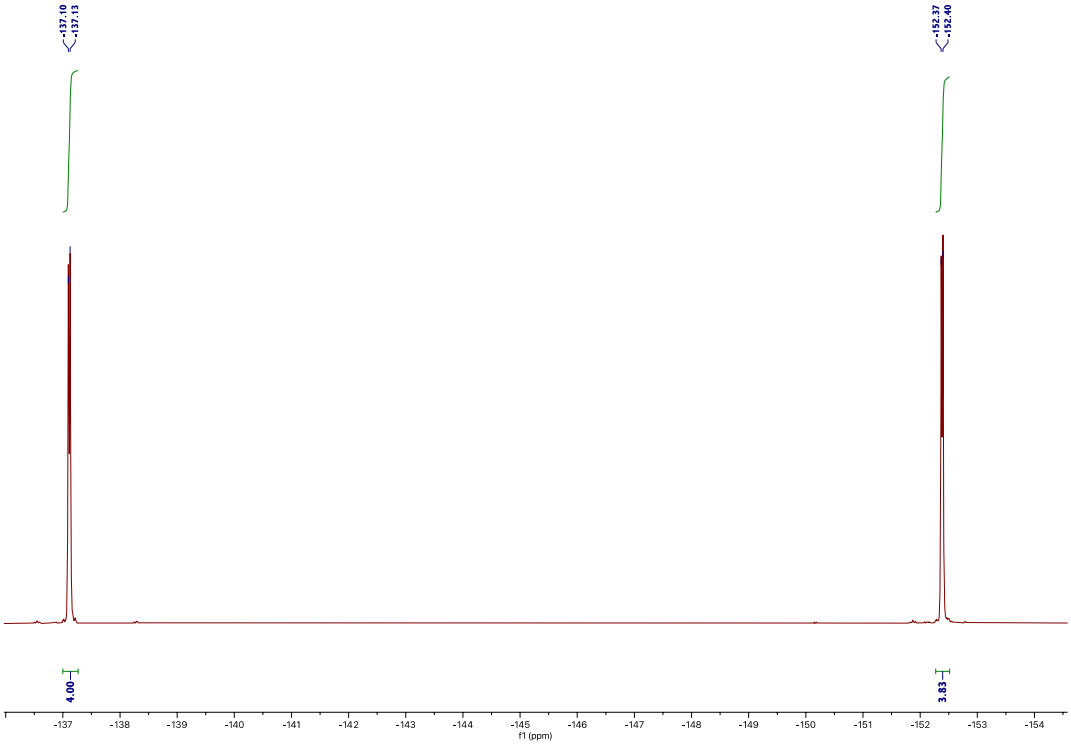

Figure S4. ^{19}F NMR spectrum of **4** in $CDCl_3$ (376.7 MHz).

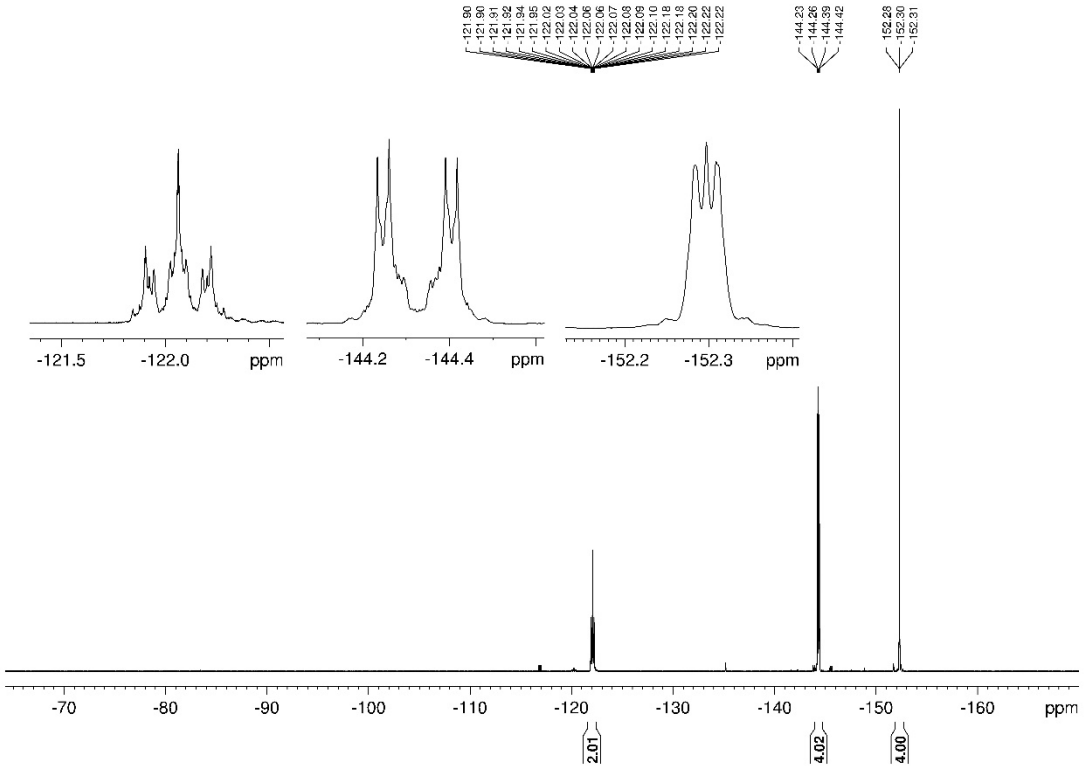

Figure S5. ^{19}F NMR spectrum of **DFA** in $CDCl_3$ (470.6 MHz).

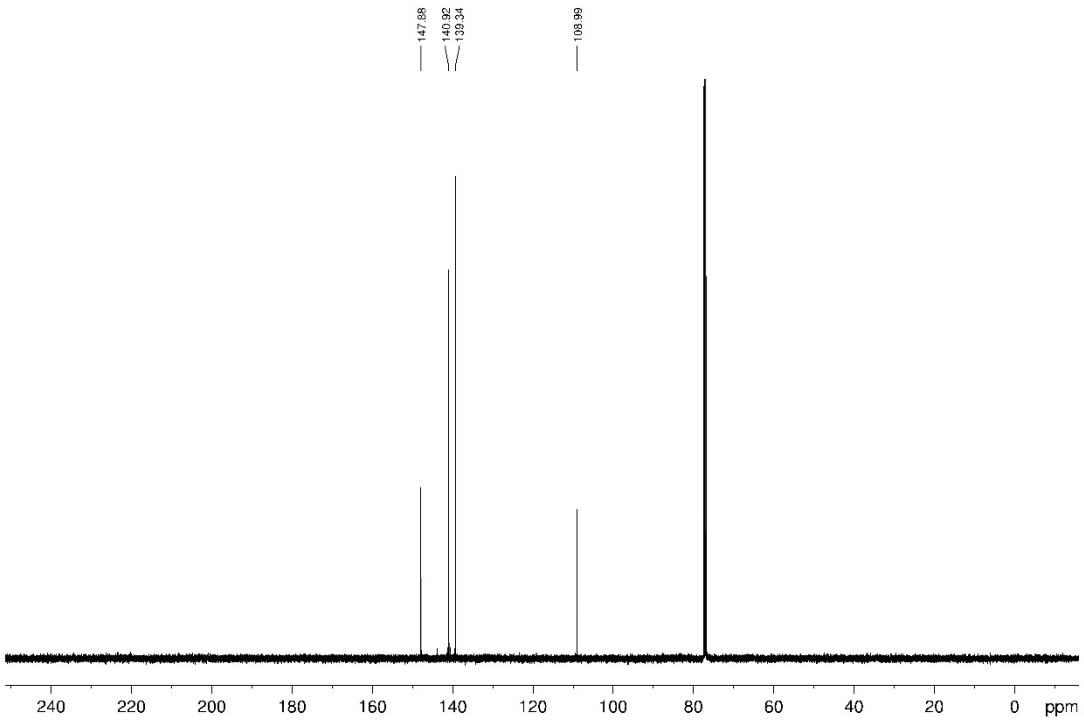

Figure S6. $^{13}C\{^{19}F\}$ NMR spectrum of **DFA** in $CDCl_3$ (125.8 MHz).

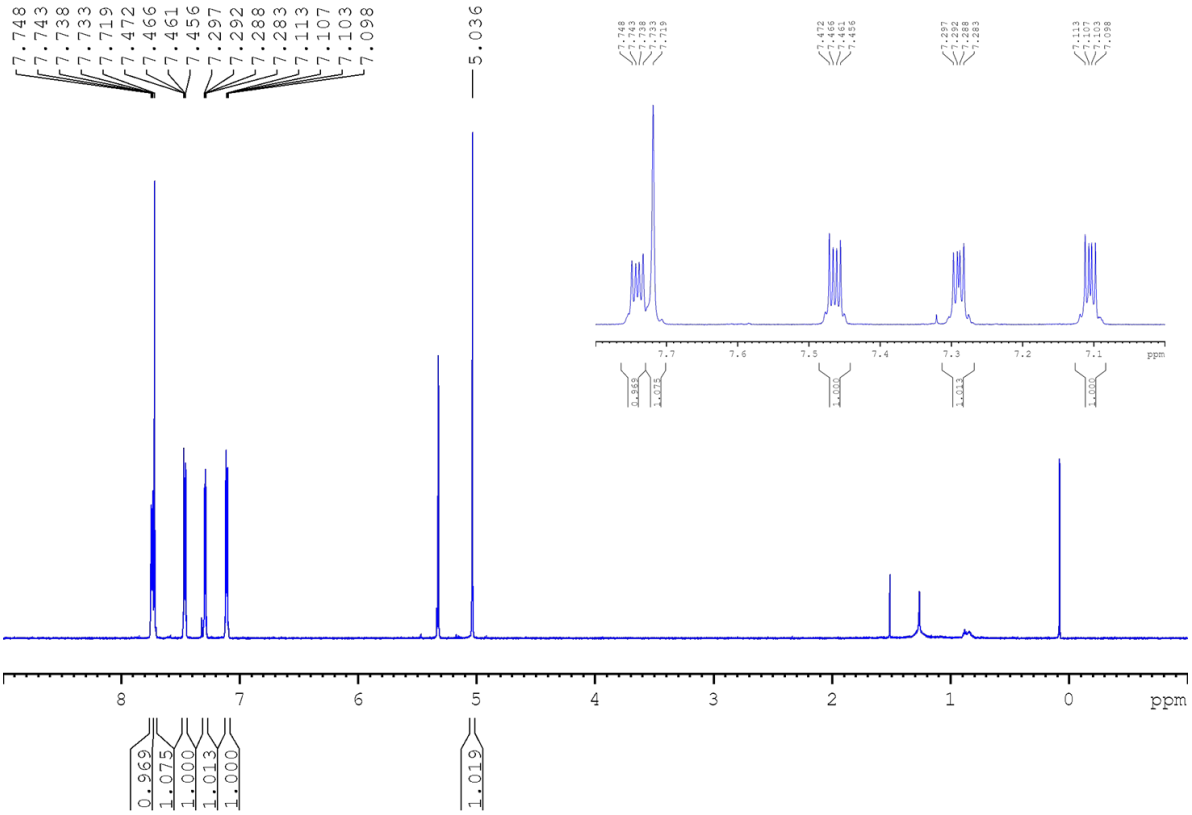

Figure S7. $^{1}H\{^{19}F\}$ NMR spectrum of **TetDFA-Dimer** in CD_2Cl_2 (600.2 MHz).

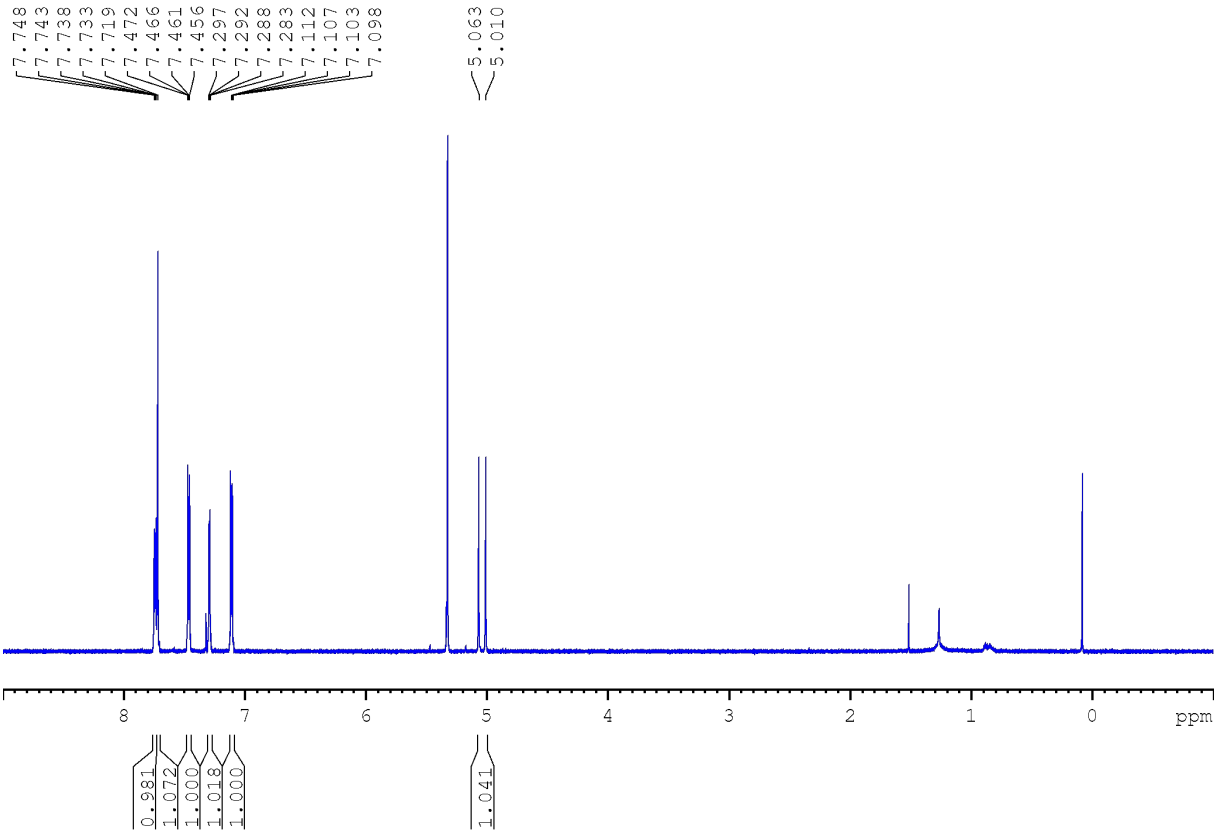

Figure S8. ^{1}H NMR spectrum of **TetDFA-Dimer** in CD_2Cl_2 (600.2 MHz).

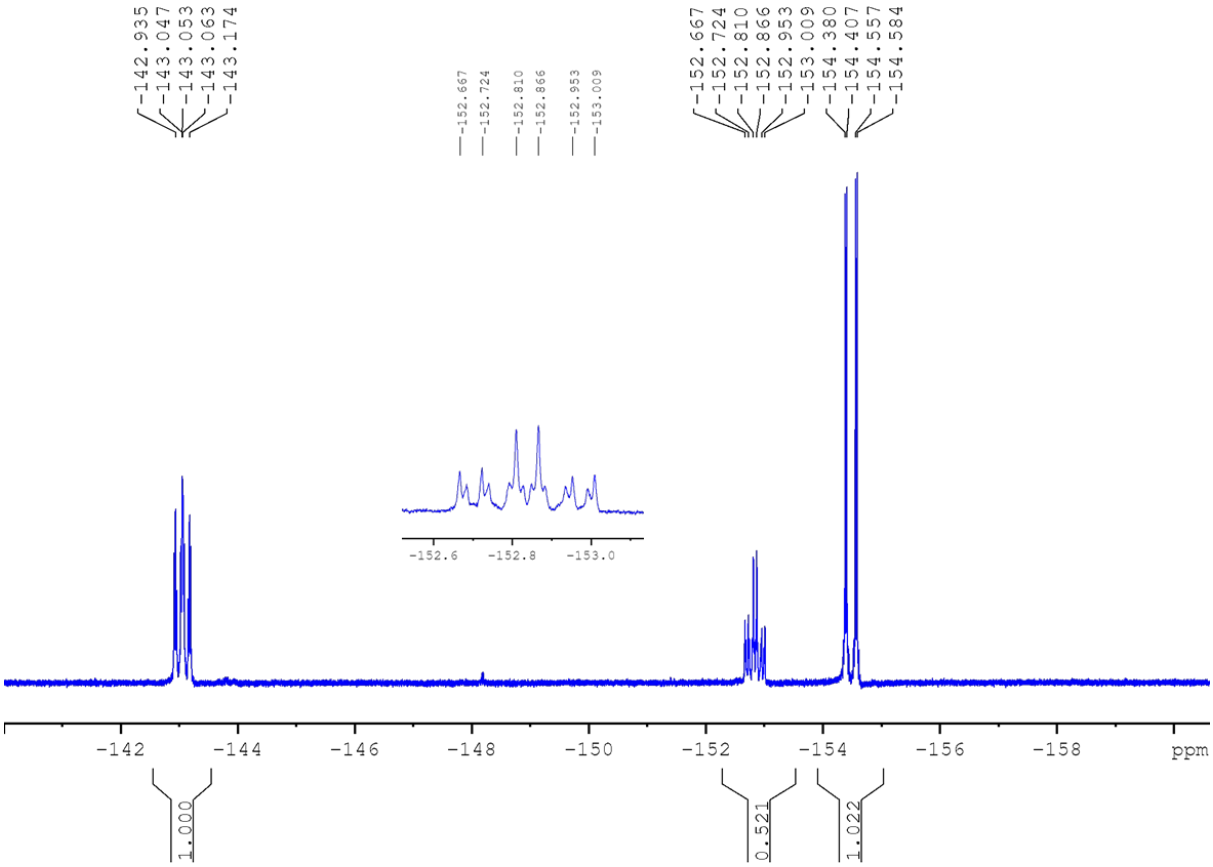

Figure S9. ^{19}F NMR spectrum of **TetDFA-Dimer** in CD_2Cl_2 (564.8 MHz).

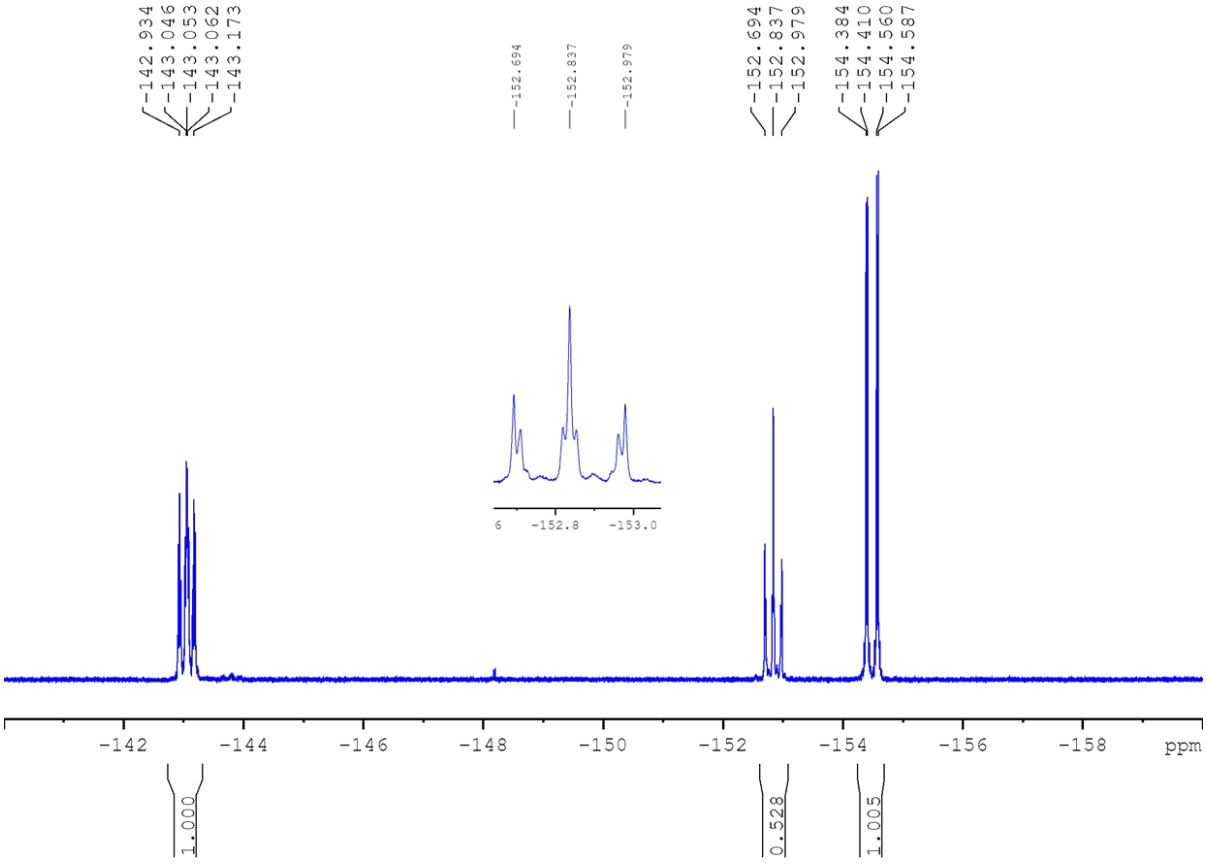

Figure S10. $^{19}F\{^1H\}$ NMR spectrum of **TetDFA-Dimer** in CD_2Cl_2 (564.8 MHz).

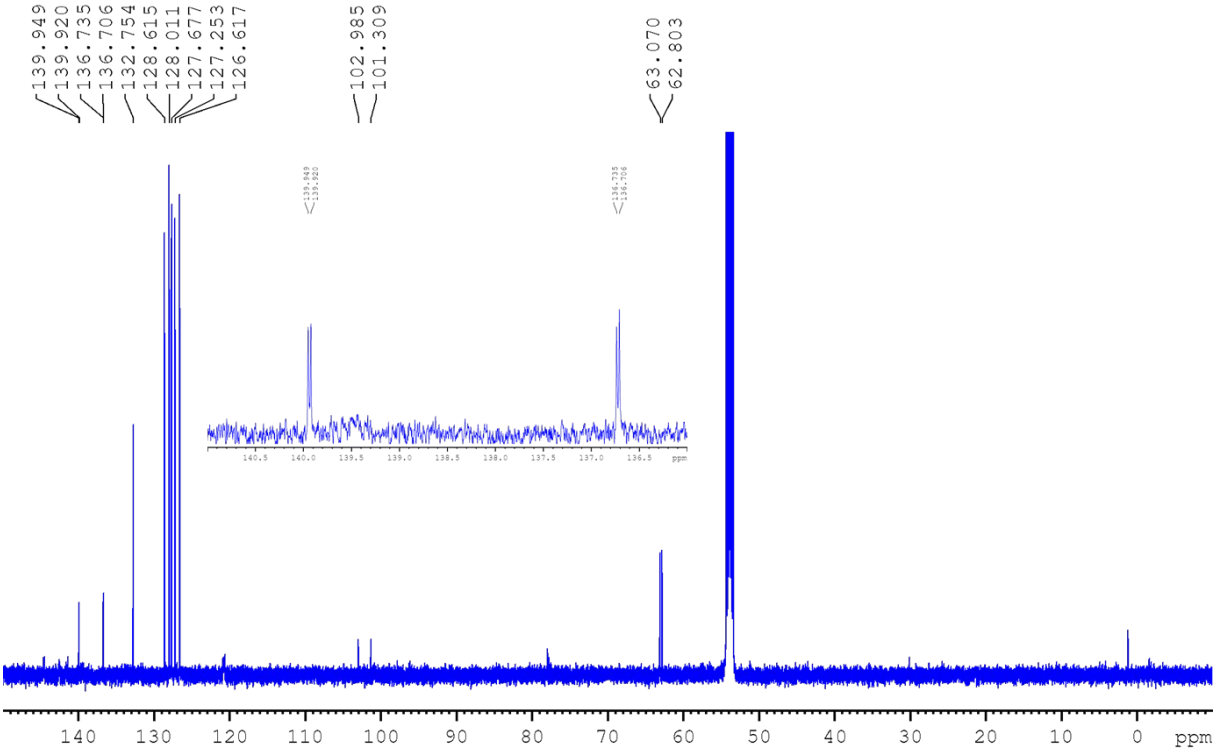

Figure S11. $^{13}C\{^{1}H\}$ NMR spectrum of **TetDFA-Dimer** in CD_2Cl_2 (125.8 MHz).

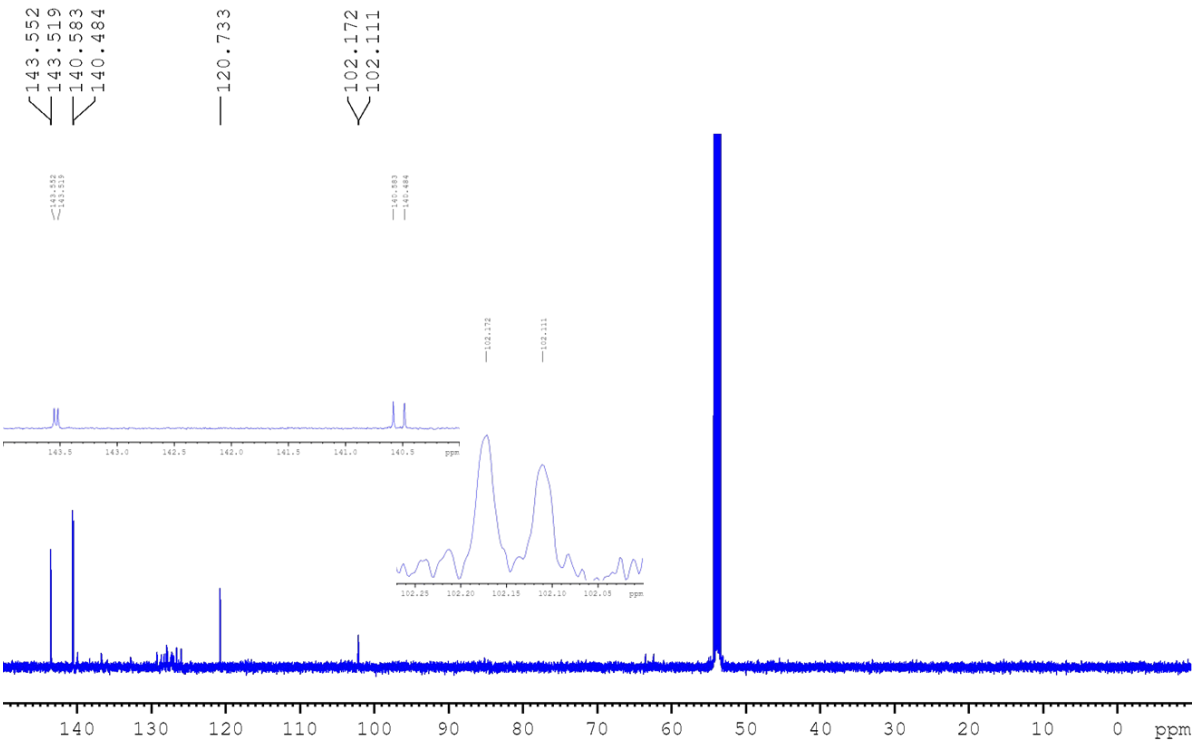

Figure S12. $^{13}C\{^{19}F\}$ NMR spectrum of **TetDFA-Dimer** in CD_2Cl_2 (125.8 MHz).

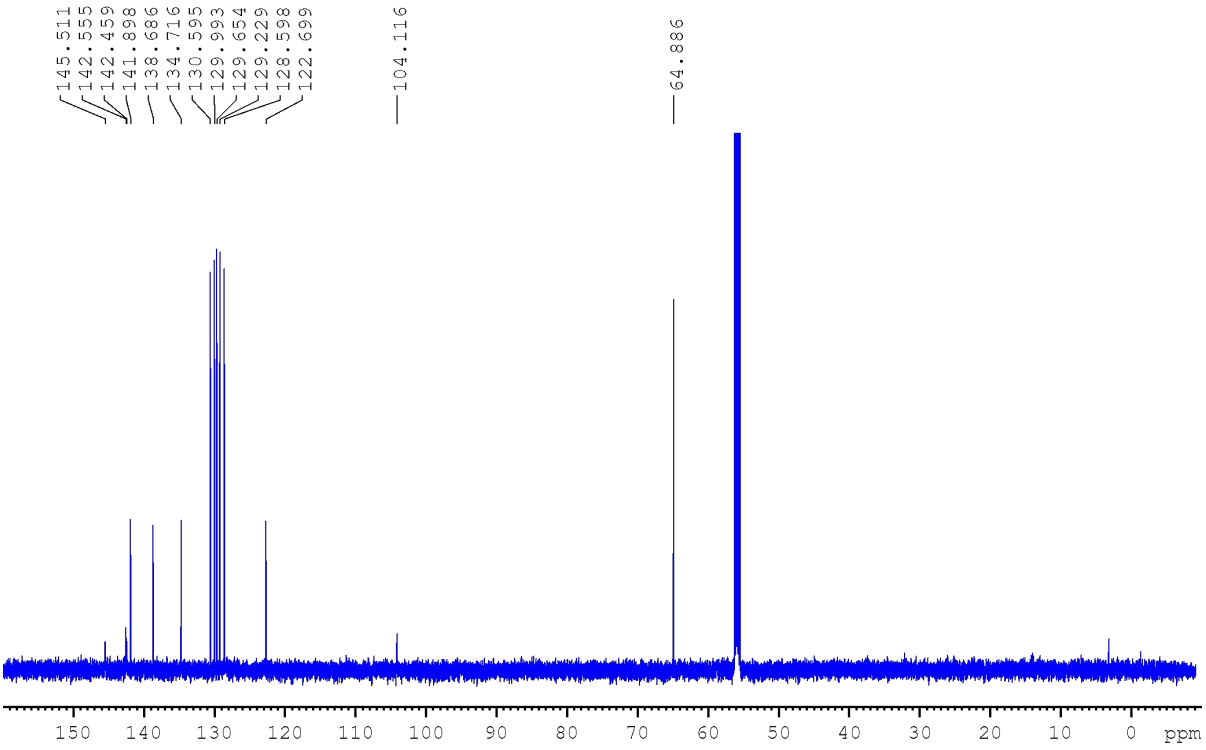

Figure S13. $^{13}C\{^{1}H,^{19}F\}$ NMR spectrum of **TetDFA-Dimer** in CD_2Cl_2 (150.9 MHz).

IV. Photophysical properties

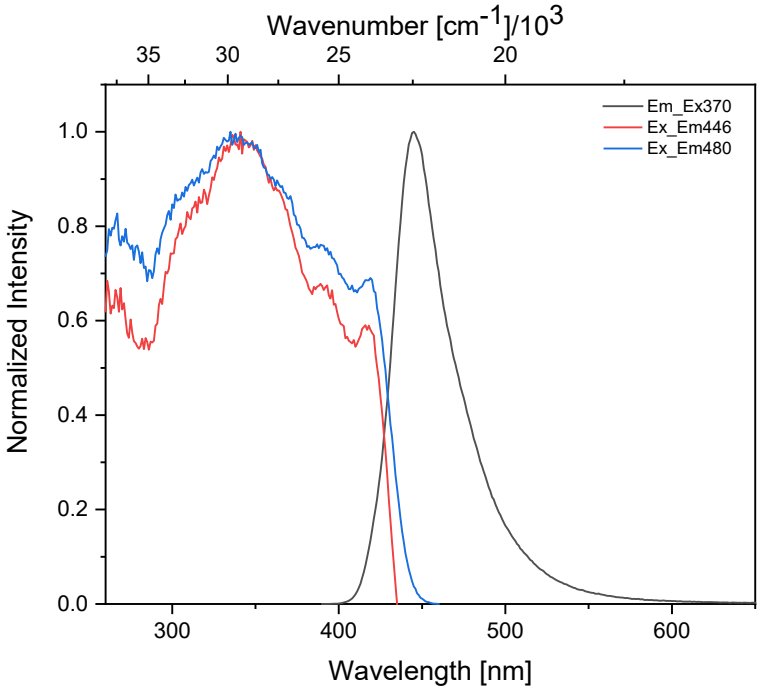

Figure S14. Excitation (blue and red) and emission (black) spectra of **DFA** in the solid state. The upper axis refers only to the excitation spectra, as the emission spectra were not corrected for display in the energy scale.[18, 19]

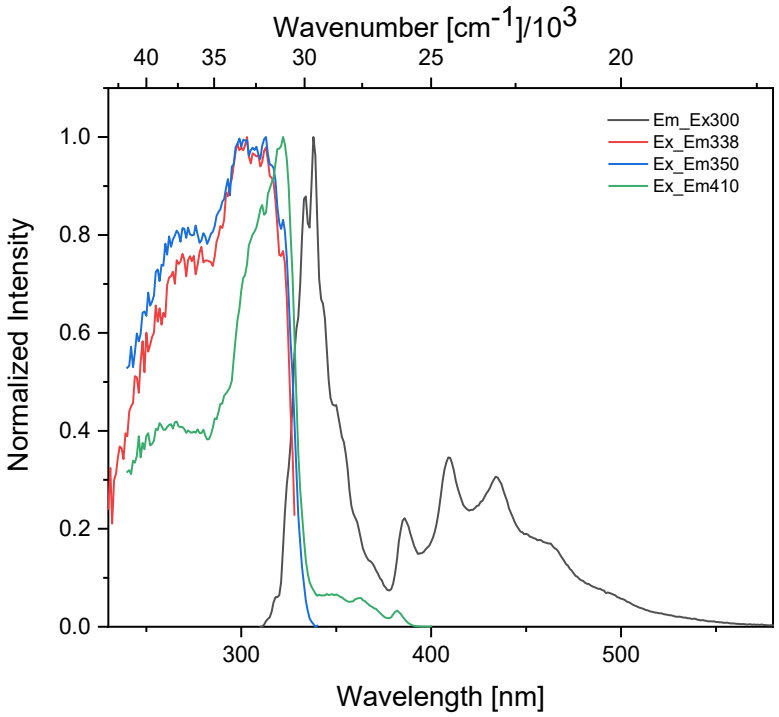

Figure S15. Excitation (blue, red and green) and emission (black) spectra of **Naphthalene** in the solid state. The upper axis refers only to the excitation spectra, see Figure S14.

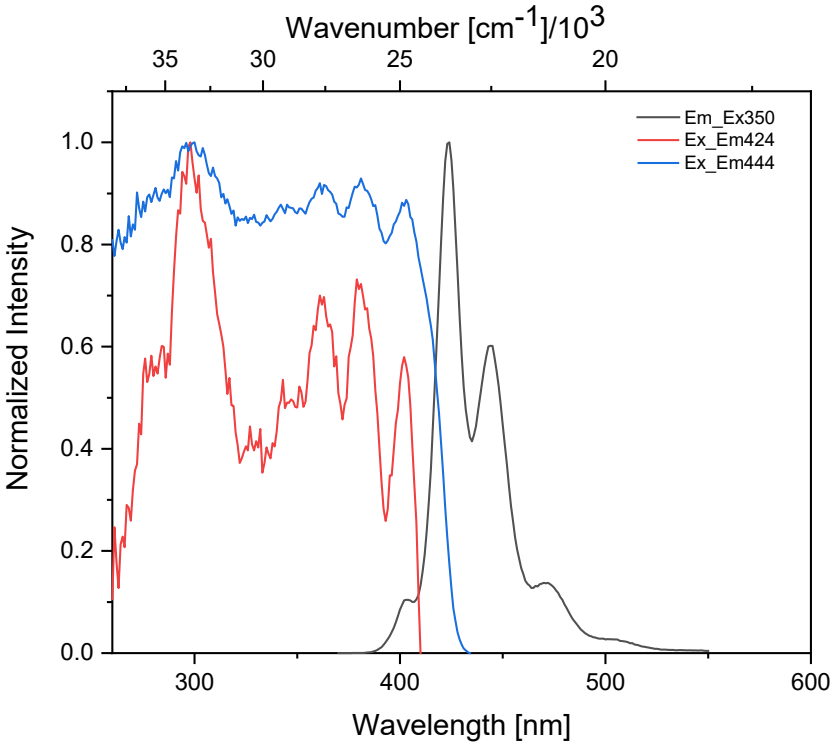

Figure S16. Excitation (blue and red) and emission (black) spectra of **Anthracene** in the solid state. The upper axis refers only to the excitation spectra, see Figure S14.

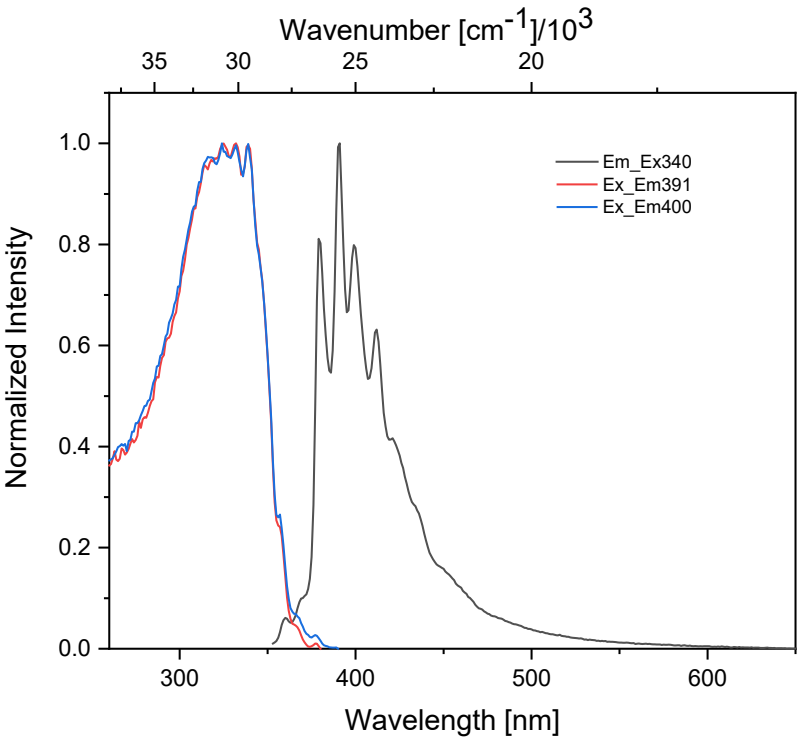

Figure S17. Excitation (blue and red) and emission (black) spectra of **Triphenylene** in the solid state. The upper axis refers only to the excitation spectra, see Figure S14.

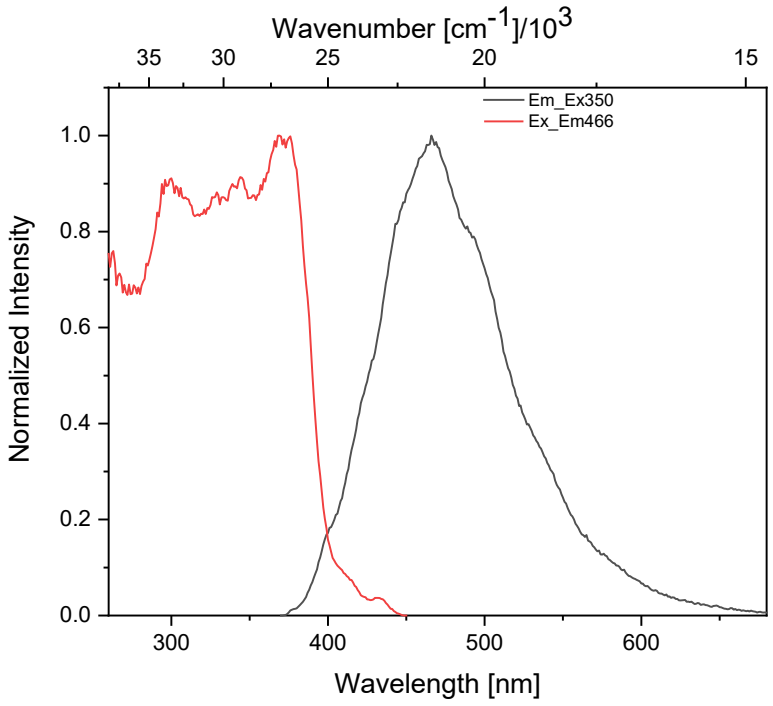

Figure S18. Excitation (red) and emission (black) spectra of **Pyrene** in the solid state. The upper axis refers only to the excitation spectrum, see Figure S14.

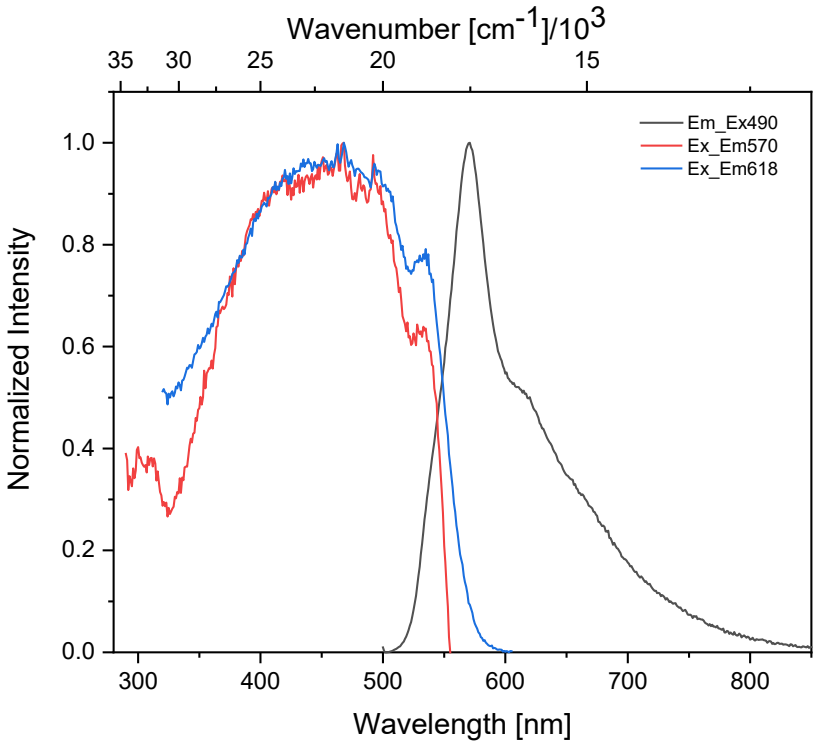

Figure S19. Excitation (blue and red) and emission (black) spectra of **Tetracene** in the solid state. The upper axis refers only to the excitation spectra, see Figure S14.

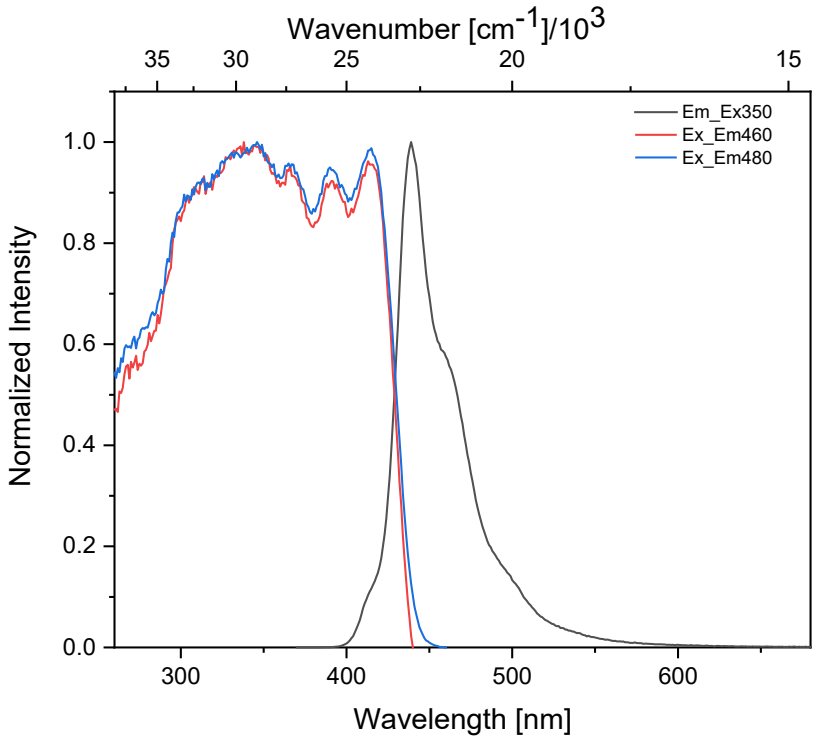

Figure S20. Excitation (blue and red) and emission (black) spectra of **NDFA** in the solid state. The upper axis refers only to the excitation spectra, see Figure S14.

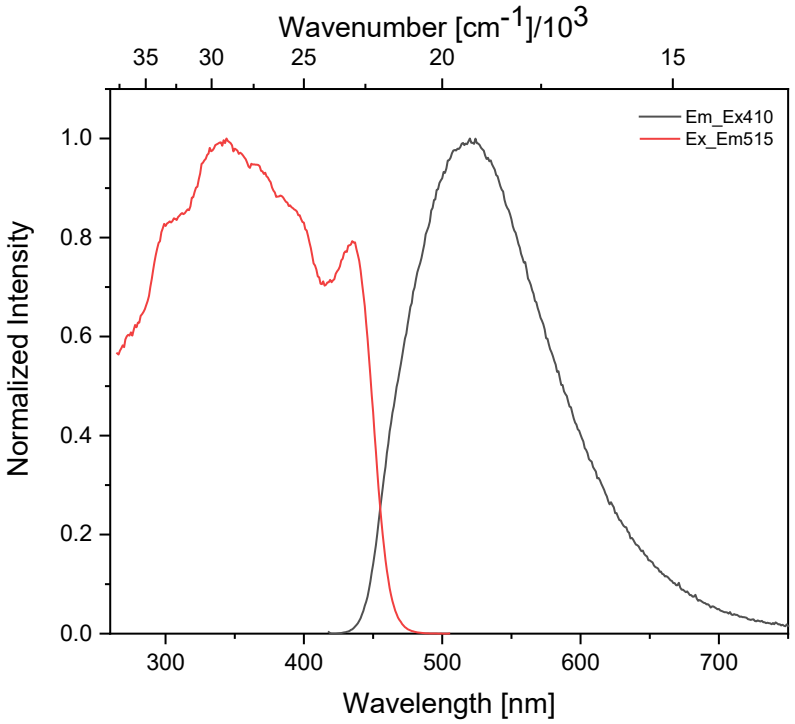

Figure S21. Excitation (red) and emission (black) spectra of **ADFA** in the solid state. The upper axis refers only to the excitation spectrum, see Figure S14.

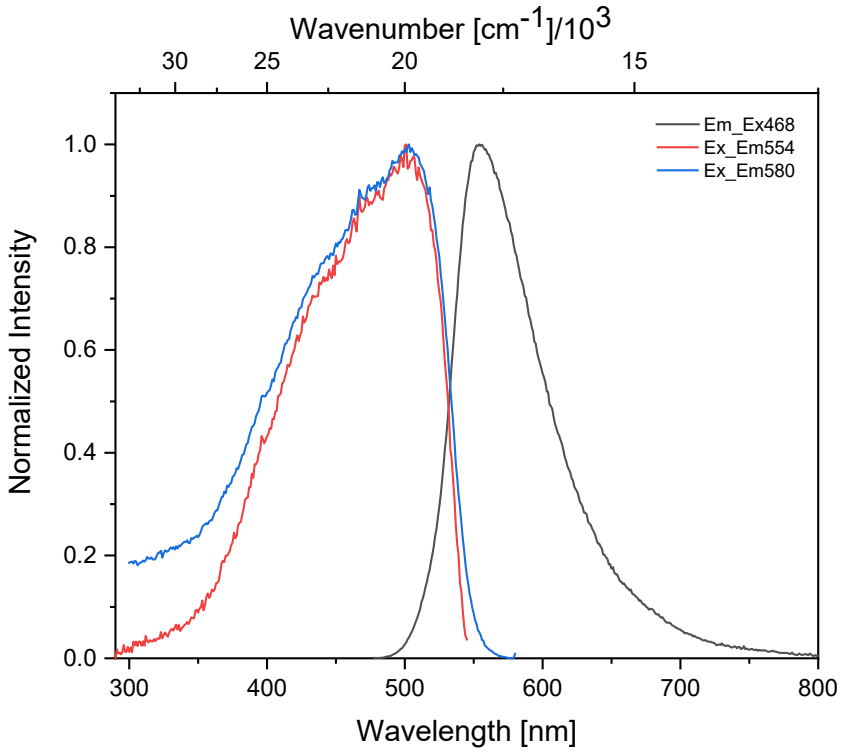

Figure S22. Excitation (blue and red) and emission (black) spectra of **TetDFA** in the solid state. The upper axis refers only to the excitation spectra, see Figure S14.

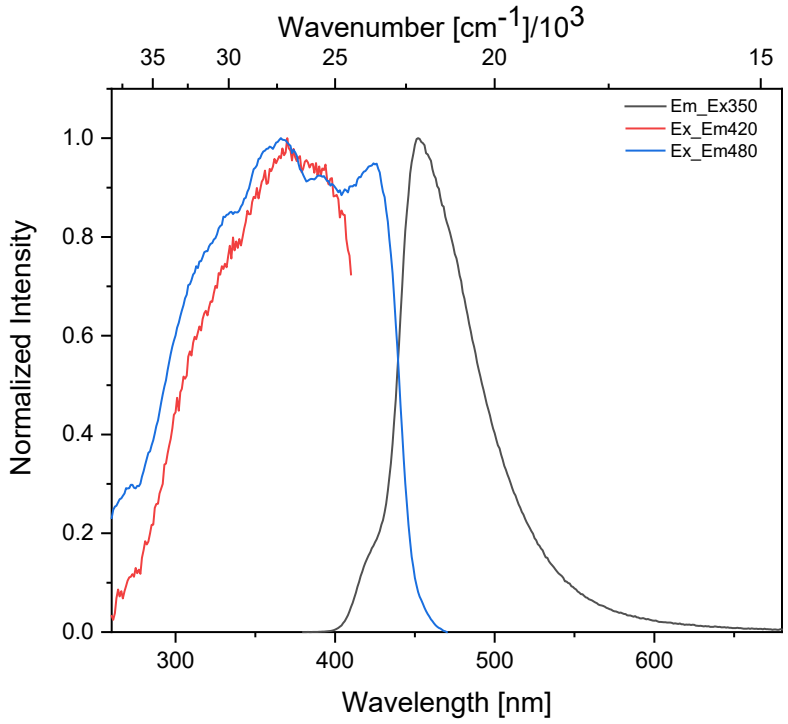

Figure S23. Excitation (blue and red) and emission (black) spectra of **PyrDFA** in the solid state. The upper axis refers only to the excitation spectra, see Figure S14.

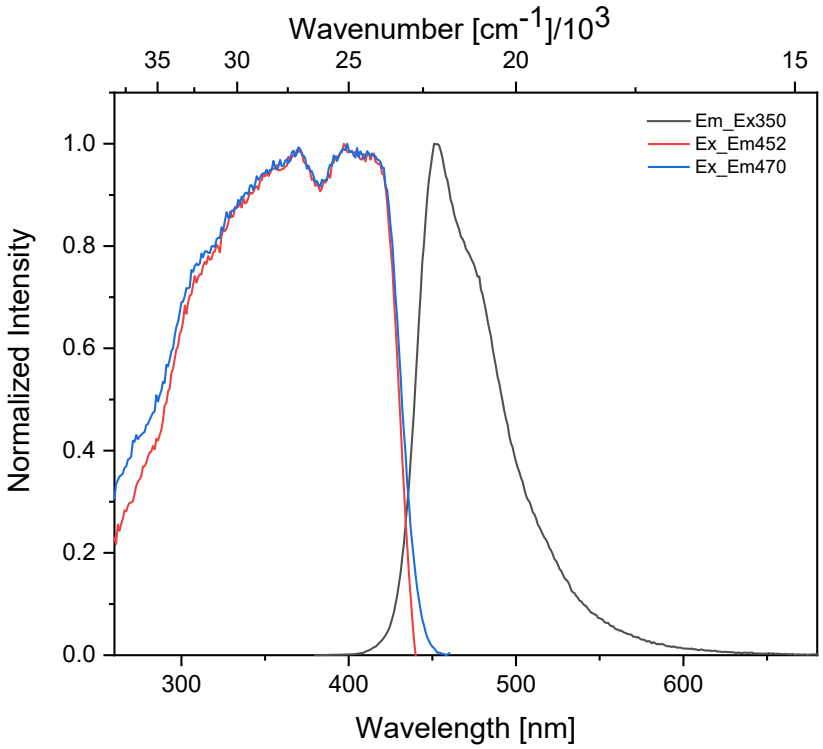

Figure S24. Excitation (blue and red) and emission (black) spectra of **TriDFA** in the solid state. The upper axis refers only to the excitation spectra, see Figure S14.

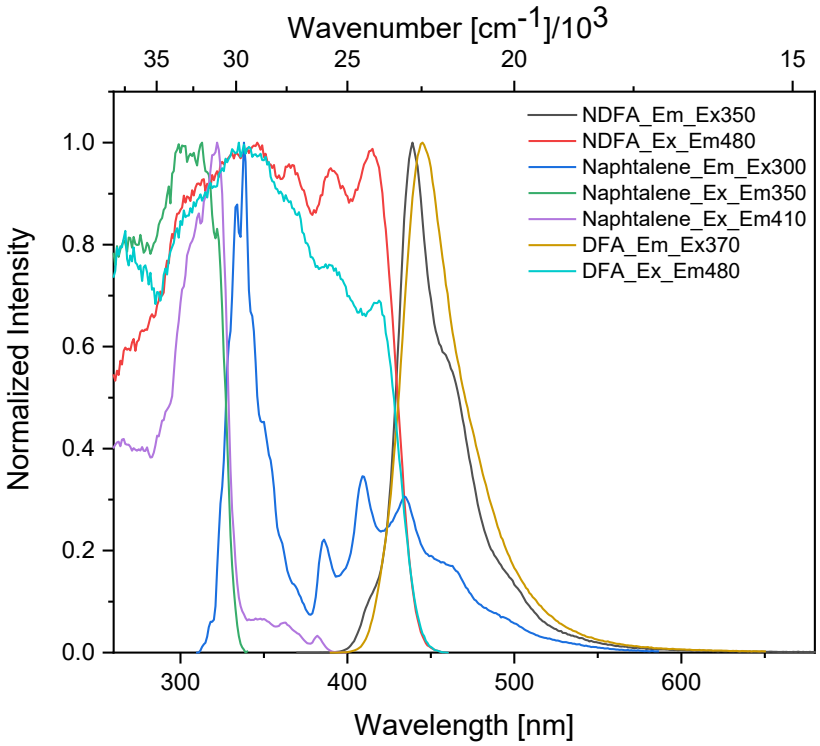

Figure S25. Excitation and emission spectra of **NDFA** and its components **Naphtalene** and **DFA** in the solid state. The upper axis refers only to the excitation spectra, see Figure S14.

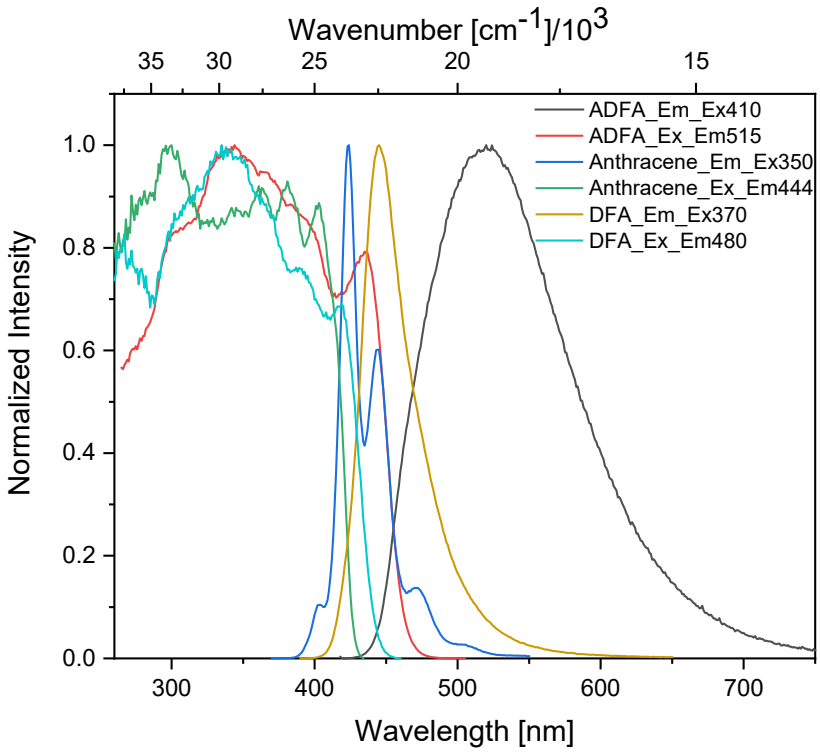

Figure S26. Excitation and emission spectra of **ADFA** and its components **Anthracene** and **DFA** in the solid state. The upper axis refers only to the excitation spectra, see Figure S14.

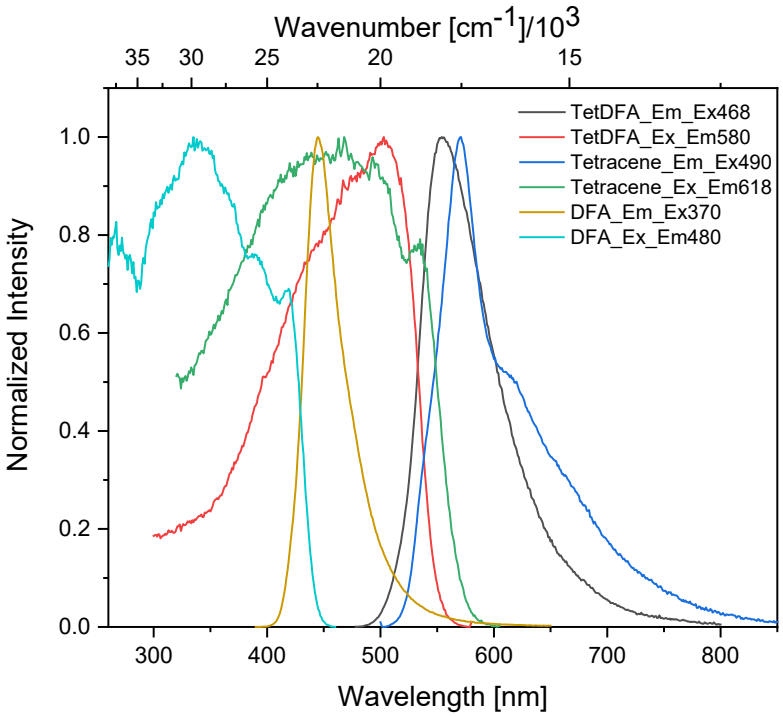

Figure S27. Excitation and emission spectra of **TetDFA** and its components **Tetracene** and **DFA** in the solid state. The upper axis refers only to the excitation spectra, see Figure S14.

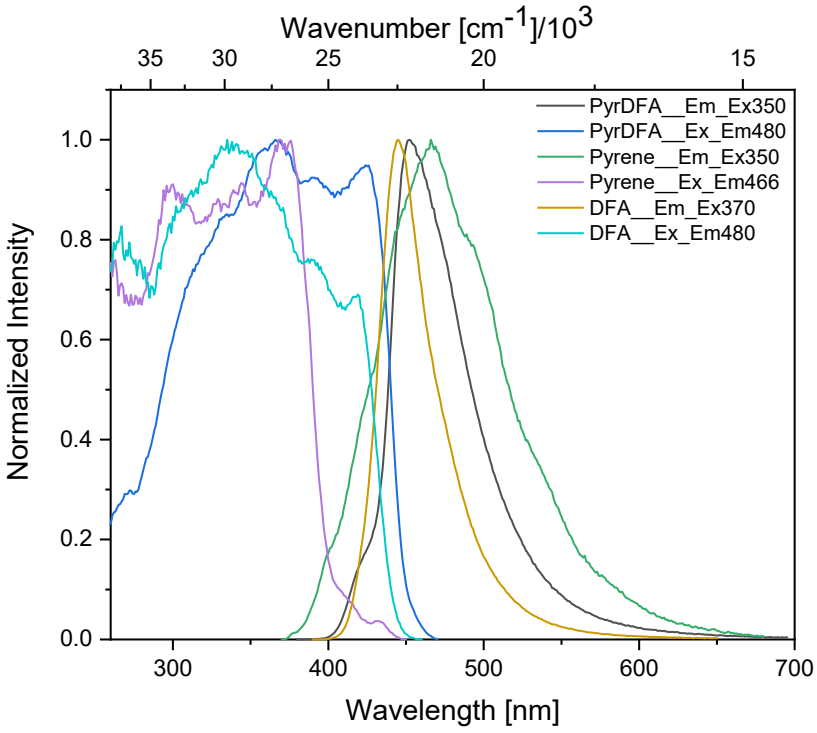

Figure S28. Excitation and emission spectra of **PyrDFA** and its components **Pyrene** and **DFA** in the solid state. The upper axis refers only to the excitation spectra, see Figure S14.

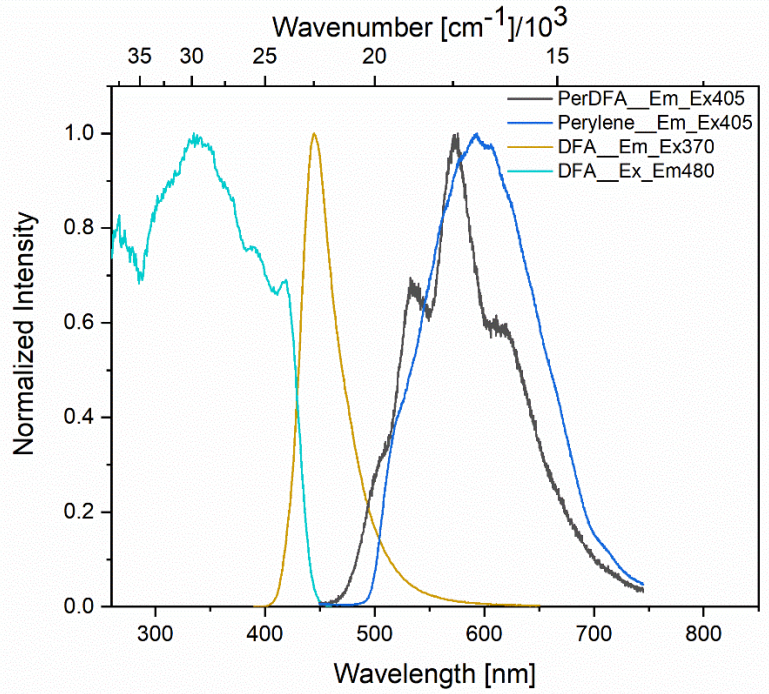

Figure S29. Emission spectra of **PerDFA** and its components **Perylene** and **DFA** and excitation spectra of **DFA** in the solid state. The upper axis refers only to the excitation spectra, see Figure S14.

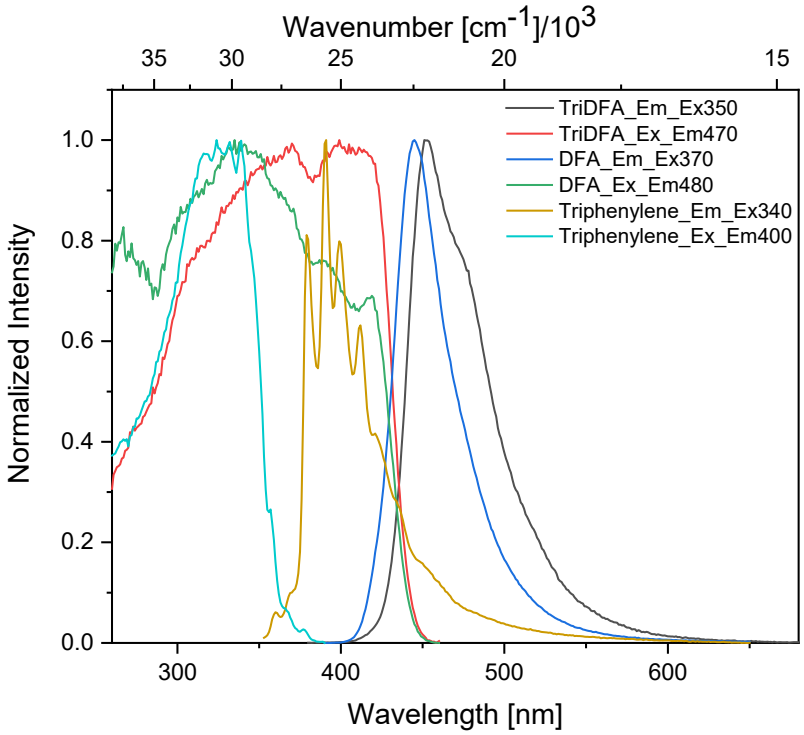

Figure S30. Excitation and emission spectra of **TriDFA** and its components **Triphenylene** and **DFA** in the solid state. The upper axis refers only to the excitation spectra, see Figure S14.

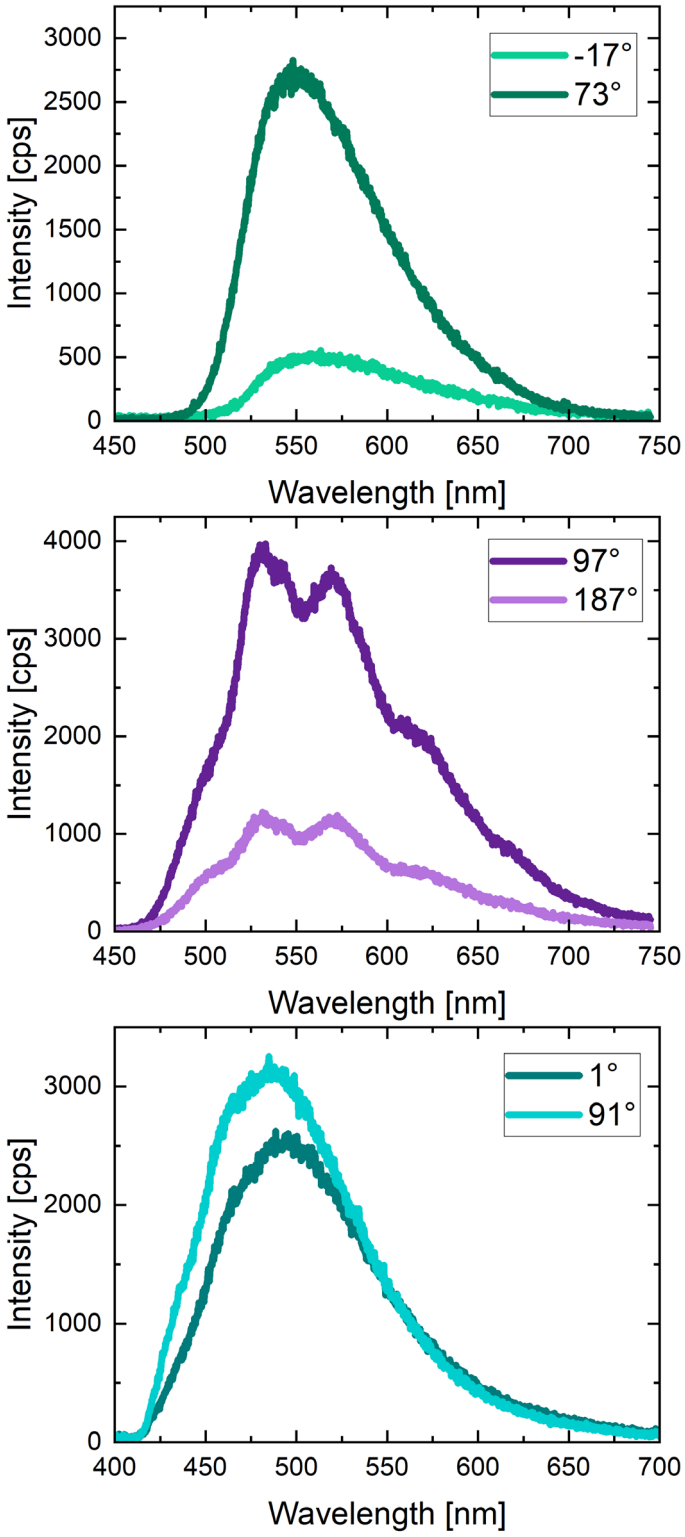

Figure S31. Emission spectra of the polarisation directions of highest and lowest intensity of **TetDFA** (top), **PerDFA** (center), and **ADFA** (bottom) in the solid state.

V. Single-crystal X-ray diffraction

Table S1. Single-crystal X-ray diffraction data and structure refinements of **DFA**, **NDFA**, **ADFA**, **TetDFA**, **TetDFA-Dimer**, **PyrDFA**, **PerDFA**, and **TriDFA** at 100 K.

	DFA (*β*-phase)[a]	**NDFA**	**ADFA**[a]	**TetDFA**
CCDC	2293625	2293626	2293628	2293631
Empirical formula	$C_{14}F_{10}$	$C_{14}F_{10} \cdot C_{10}H_8$	$C_{14}F_{10} \cdot C_{14}H_{10}$	$C_{14}F_{10} \cdot C_{18}H_{12}$
M / g·mol^{-1}	358.14	486.30	536.36	586.42
T / K	100(2)	100(2)	100(2)	100(2)
Radiation, λ / Å	Cu K_α, 1.54184	Cu K_α, 1.54184	CuK_α, 1.54184	CuK_α, 1.54184
Crystal size/mm^3	0.05×0.19×0.27	0.02×0.27×0.34	0.02×0.05×0.30	0.02×0.05×0.12
Crystal colour, habit	colourless plate	colourless plate	colourless needle	orange plate
Crystal system	monoclinic	monoclinic	triclinic	triclinic
Space group	$P2_1/c$	$P2_1/n$	$P\bar{1}$	$P\bar{1}$
a / Å	21.8459(5)	7.4096(2)	7.0884(3)	6.9115(2)
b / Å	4.54869(9)	6.5845(2)	7.3423(2)	7.1394(3)
c / Å	11.3393(2)	18.7792(6)	10.3604(3)	12.1965(5)
α / °	90	90	85.427(3)	80.570(3)
β / °	103.937(2)	96.356(3)	74.157(3)	73.691(3)
γ / °	90	90	78.753(3)	84.021(3)
Volume / Å^3	1093.61(4)	910.57(5)	508.56(3)	568.73(4)
Z	4	2	1	1
ρ_{calc} / g·cm^{-3}	2.175	1.774	1.751	1.712
μ / mm^{-1}	2.282	1.569	1.475	1.383
F(000)	696	484	268	294
θ range / °	4.170–74.451	6.215–74.945	4.438–74.487	3.814–74.390
Reflections collected	11895	12566	10583	11621
Unique reflections	2209	2878	2073	2295
Parameters	218	155	172	190
GooF on F^2	1.074	1.125	1.071	1.062
R_1 [$I \geq 2\sigma$ (I)]	0.0410	0.0538	0.0344	0.0385
wR_2 [all data]	0.1215	0.1749	0.1055	0.1100
Max. / min. residual electron density/ e·Å^{-3}	0.27/-0.22	0.29/–0.36	0.265 / –0.250	0.20/-0.29

[a] The crystal structures of the *β*-polymorph of DFA at 173 K (CCDC 2089979) and of ADFA at 184 K (CCDC 1581425) were reported earlier by Bischof et al. (2021).[20]

Table S1. continued.

	TetDFA-Dimer	**PyrDFA**	**PerDFA**	**TriDFA**
CCDC	2293633	2293635	2293637	2293638
Empirical formula	$C_{32}H_{12}F_{10}$	$C_{14}F_{10} \cdot C_{16}H_{10}$	$C_{14}F_{10} \cdot C_{20}H_{12}$	$C_{14}F_{10} \cdot C_{18}H_{12}$
M / g·mol^{-1}	586.42	560.38	610.44	586.42
T / K	100(2)	100(2)	100(2)	100(2)
Radiation, λ / Å	CuK$_\alpha$, 1.54184	Cu-K$_\alpha$ 1.54184	CuK$_\alpha$, 1.54184	Cu-K$_\alpha$, 1.54184
Crystal size/mm^3	0.05×0.13×0.39	0.05×0.15×0.19	0.02×0.08×0.51	0.06×0.07×0.40
Crystal colour, habit	colourless plate	colourless plate	yellow plate	colourless needle
Crystal system	triclinic	monoclinic	triclinic	Monoclinic
Space group	$P\bar{1}$	$P2_1/c$	$P\bar{1}$	$P2_1/n$
a / Å	9.9708(3)	7.1553(2)	6.9692(5)	6.71719(9)
b / Å	10.0237(4)	8.5840(2)	8.9198(6)	37.6558(5)
c / Å	12.7358(5)	17.2031(4)	10.9187(8)	9.27231(15)
α / °	70.185(4)	90	66.146(7)	90
β / °	77.145(3)	91.246(2)	87.489(6)	101.9071(15)
γ / °	85.923(3)	90	71.797(6)	90
Volume / Å^3	1167.48(8)	1056.38(5)	587.03(8)	2294.88(6)
Z	2	2	1	4
ρ_{calc} / g·cm^{-3}	1.668	1.762	1.727	1.697
μ / mm^{-1}	1.347	1.455	1.370	1.371
F(000)	588	560	306	1176
θ range / °	3.774–74.319	5.143–74.467	4.448–73.702	2.347–74.493
Reflections collected	23759	11099	11572	24608
Unique reflections	4668	2140	2334	4698
Parameters	380	181	199	380
GooF on F^2	1.058	1.059	1.008	1.052
R_1 [$I \geq 2\sigma(I)$]	0.0326	0.0398	0.0693	0.0339
wR_2 [all data]	0.0913	0.1155	0.2085	0.1002
Max. / min. residual electron density/ e·Å^{-3}	0.27/-0.21	0.241 / –0.263	0.59 / –0.43	0.26 / –0.21

Table S2. Single-crystal X-ray diffraction data and structure refinements of **NDFA**, **ADFA**, **TetDFA**, **TetDFA-Dimer**, **PyrDFA**, and **TriDFA** at ambient temperature, and of **ADFA** at 200 K.

	NDFA	**ADFA**	**ADFA**	**TetDFA**
CCDC	2293627	2293630	2293629	2293632
Empirical formula	$C_{14}F_{10} \cdot C_{10}H_8$	$C_{14}F_{10} \cdot C_{14}H_{10}$	$C_{14}F_{10} \cdot C_{14}H_{10}$	$C_{14}F_{10} \cdot C_{18}H_{12}$
M / g·mol^{-1}	486.30	536.36	536.36	586.42
T / K	299(2)	299(2)	200(2)	298(2)
Radiation, λ / Å	Cu K_α, 1.54184	CuK$_\alpha$, 1.54184	CuK$_\alpha$, 1.54184	CuK$_\alpha$, 1.54184
Crystal size/mm^3	0.12×0.17×0.33	0.05×0.22×0.32	0.05×0.07×0.36	0.02×0.06×0.14
Crystal colour, habit	colourless plate	colourless plate	colourless needle	orange plate
Crystal system	monoclinic	triclinic	triclinic	triclinic
Space group	$P2_1/n$	$P\bar{1}$	$P\bar{1}$	$P\bar{1}$
a / Å	7.5869(2)	7.2524(3)	7.14326(18)	7.0122(4)
b / Å	6.63558(18)	7.4269(4)	7.39508(19)	7.2711(4)
c / Å	19.0089(6)	10.5461(6)	10.4097(3)	12.2638(6)
α / °	90	83.280(4)	84.893(2)	79.844(4)
β / °	97.108(3)	73.176(5)	73.918(2)	73.405(4)
γ / °	90	77.567(4)	78.314(2)	82.693(4)
Volume / Å^3	949.62(5)	530.07(5)	517.10(3)	587.89(5)
Z	2	1	1	1
ρ_{calc} / g·cm^{-3}	1.701	1.680	1.722	1.656
μ / mm^{-1}	1.504	1.416	1.451	1.338
F(000)	484	268	268	294
θ range / °	4.689–74.460	4.387–74.058	4.423–74.408	3.802–74.270
Reflections collected	10241	10772	6934	11965
Unique reflections	1936	2123	2078	2345
Parameters	154	172	173	190
GooF on F^2	1.056	1.098	1.089	1.037
R_1 [$I \geq 2\sigma$ (I)]	0.0410	0.0692	0.0309	0.0382
wR_2 [all data]	0.1122	0.2569	0.1035	0.1189
Max. / min. residual electron density/ e·Å^{-3}	0.13/–0.19	0.36 / –0.14	0.21 / –0.16	0.14/-0.19

Table S2. continued.

	TetDFA-Dimer	**PyrDFA**	**TriDFA**
CCDC	2293634	2293636	2293639
Empirical formula	$C_{32}H_{12}F_{10}$	$C_{14}F_{10} \cdot C_{16}H_{10}$	$C_{14}F_{10} \cdot C_{18}H_{12}$
M / g·mol^{-1}	586.42	560.38	586.42
T / K	298(2)	300(2)	300(2)
Radiation, λ / Å	CuK$_\alpha$, 1.54184	Cu-K$_\alpha$, 1.54184	Cu-K$_\alpha$, 1.54184
Crystal size/mm^3	0.12×0.14×0.29	0.16×0.29×0.57	0.09×0.17×0.21
Crystal colour, habit	colourless block	colourless plate	colourless block
Crystal system	triclinic	monoclinic	monoclinic
Space group	$P\bar{1}$	$P2_1/c$	$P2_1/n$
a / Å	10.0716(3)	7.35337(14)	6.85393(13)
b / Å	10.1045(2)	8.5989(2)	37.9170(8)
c / Å	12.8392(4)	17.4368(4)	9.3367(2)
α / °	70.147(2)	90	90
β / °	76.929(3)	91.9800(19)	102.002(2)
γ / °	85.958(2)	90	90
Volume / Å^3	1197.10(6)	1101.89(4)	2373.37(9)
Z	2	2	4
ρ_{calc} / g·cm^{-3}	1.627	1.689	1.641
μ / mm^{-1}	1.314	1.395	1.325
F(000)	588	560	1176
θ range / °	3.748–74.407	5.076–74.503	2.330–74.480
Reflections collected	24611	11875	25928
Unique reflections	4784	2232	4834
Parameters	380	182	380
GooF on F^2	1.068	1.086	1.033
R_1 [$I \geq 2\sigma(I)$]	0.0333	0.0515	0.0397
wR_2 [all data]	0.0981	0.1613	0.1204
Max. / min. residual electron density/ e·Å^{-3}	0.18/-0.16	0.48 / –0.15	0.20 / –0.14

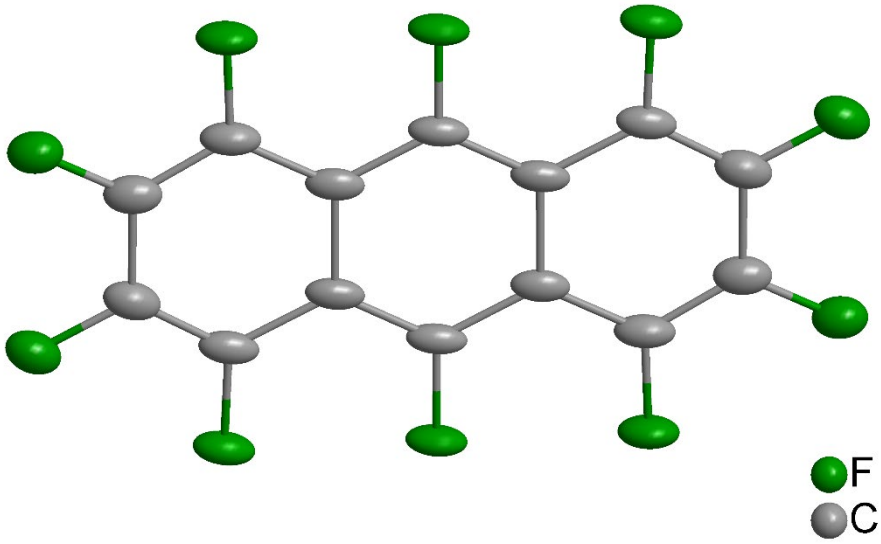

Figure S32. The solid-state molecular structure of decafluoroanthracene, **DFA**, determined by single-crystal X-ray diffraction at 100 K. All ellipsoids are drawn at the 50% probability level, and H atoms are omitted for clarity. There are two symmetry-independent molecules in the unit cell, both having inversion symmetry.

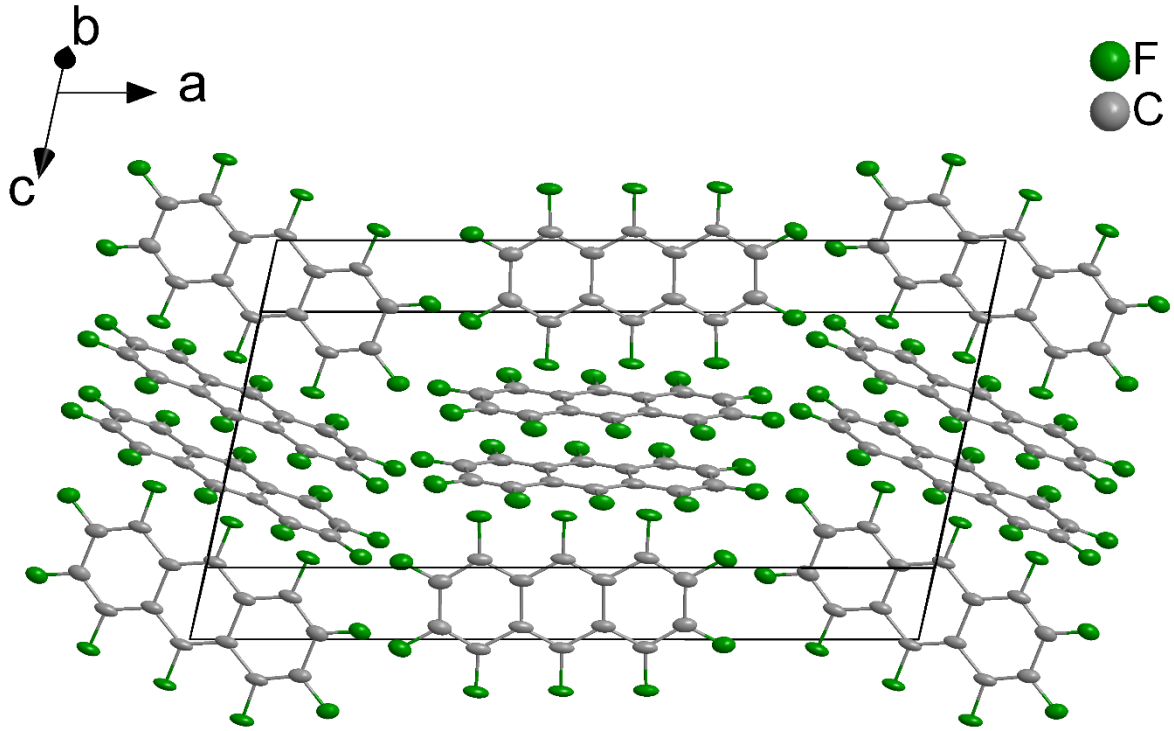

Figure S33. Crystal structure of the *β*-polymorph of decafluoroanthracene, ***β*-DFA**, showing the packing of the molecules at 100 K.

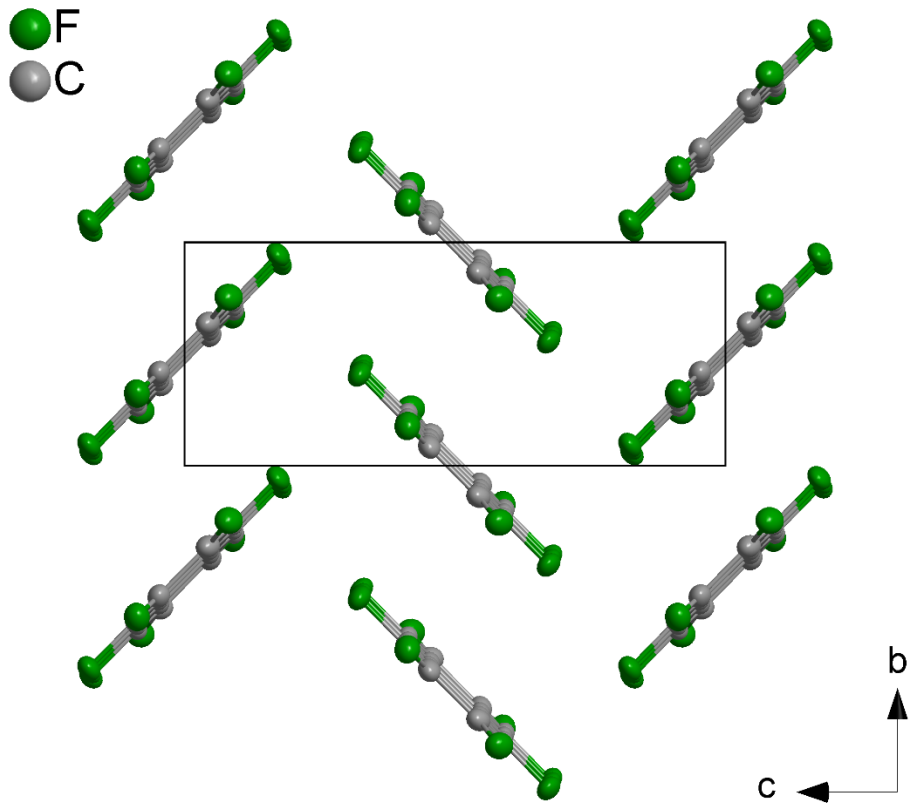

Figure S34. A slice of the crystal structure of the *β*-polymorph of decafluoroanthracene, ***β*-DFA** projected along the *a* axis showing the packing of the molecules in this sheet at 100 K.

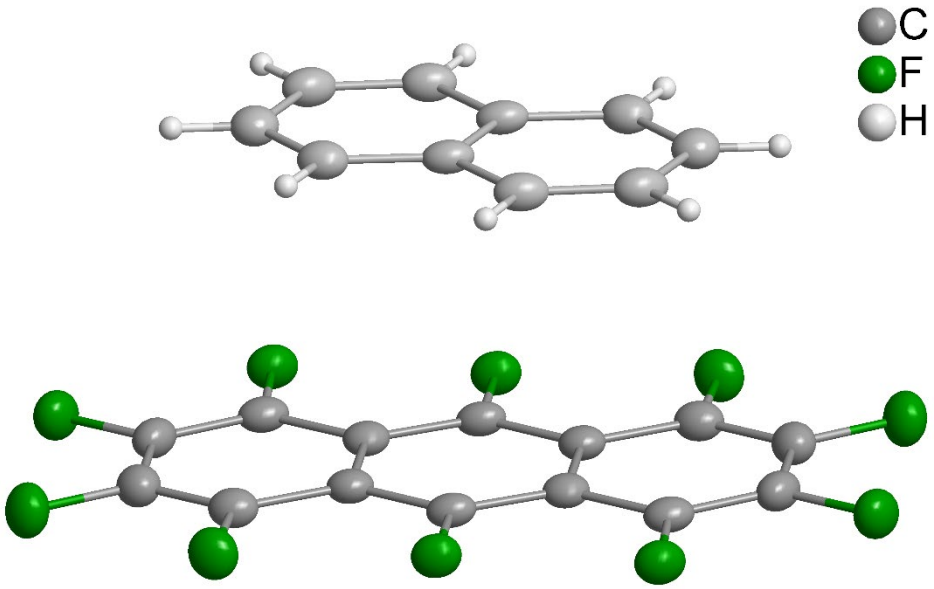

Figure S35. The solid-state molecular structure of 1:1 naphthalene:decafluoroanthracene, **NDFA**, determined by single-crystal X-ray diffraction at 100 K. All ellipsoids are drawn at the 50% probability level. Both molecules have inversion symmetry.

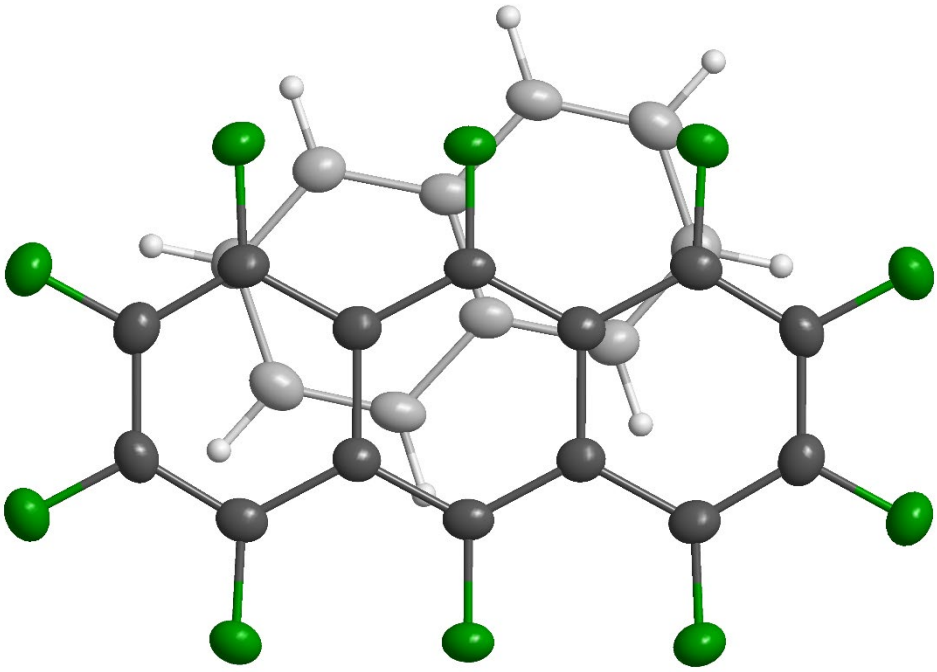

Figure S36. Molecular overlap and π-stacking of decafluoroanthracene with naphthalene viewed perpendicular to the decafluoroanthracene mean plane, at 100 K. Fluorine atoms are coloured green in decafluoroanthracene molecules.

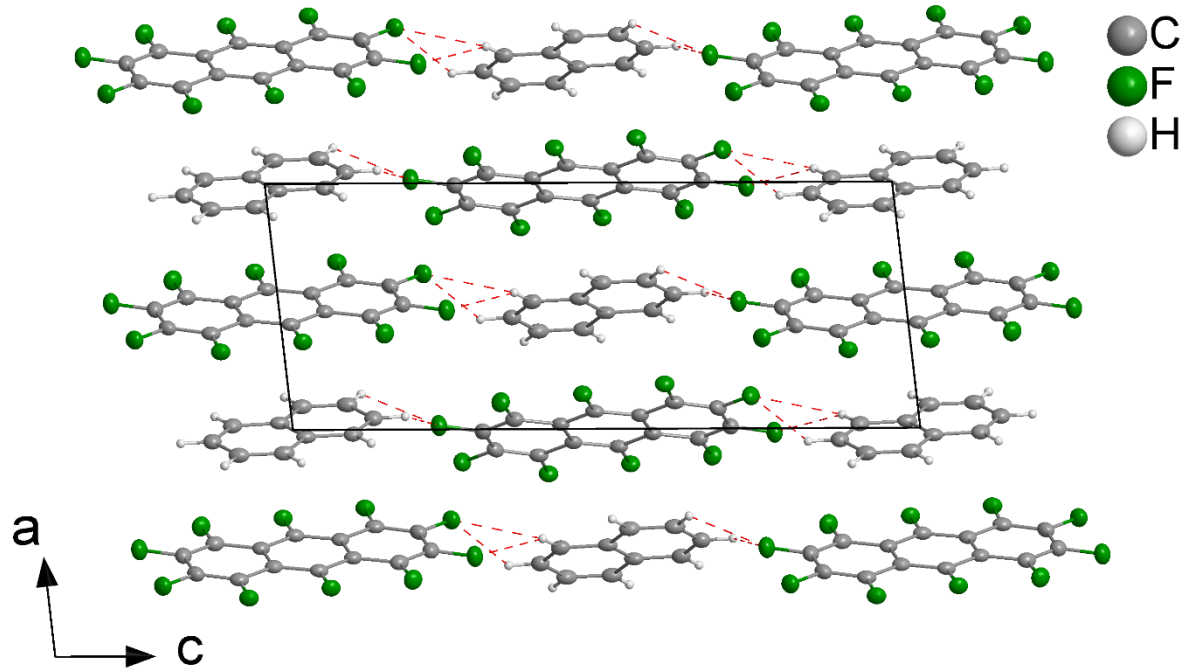

Figure S37. Packing diagram for 1:1 naphthalene:decafluoroanthracene (**NDFA**), showing the π-stacking of the components along the *a* axis at 100 K. Intermolecular H···F contacts between the stacks below the sum of the van der Waals radii are shown as red dashed lines.

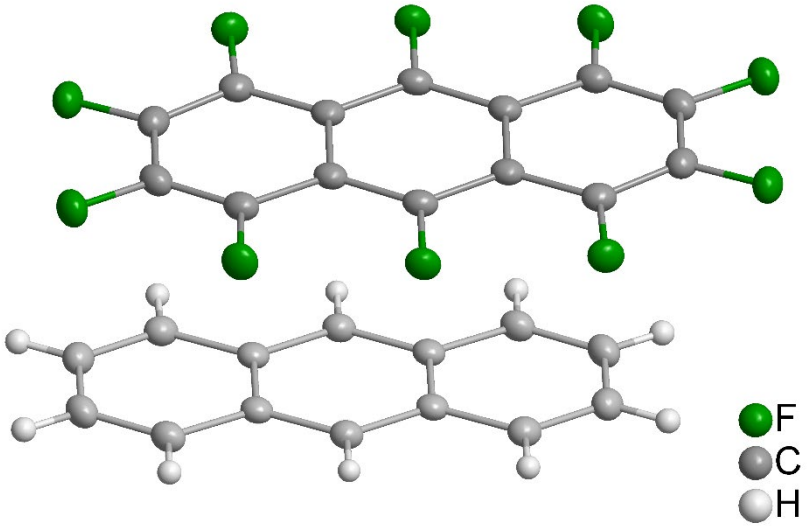

Figure S38. The solid-state molecular structure of 1:1 anthracene:decafluoroanthracene, **ADFA**, determined by single-crystal X-ray diffraction at 100 K. All ellipsoids are drawn at the 50% probability level. Both molecules have inversion symmetry.

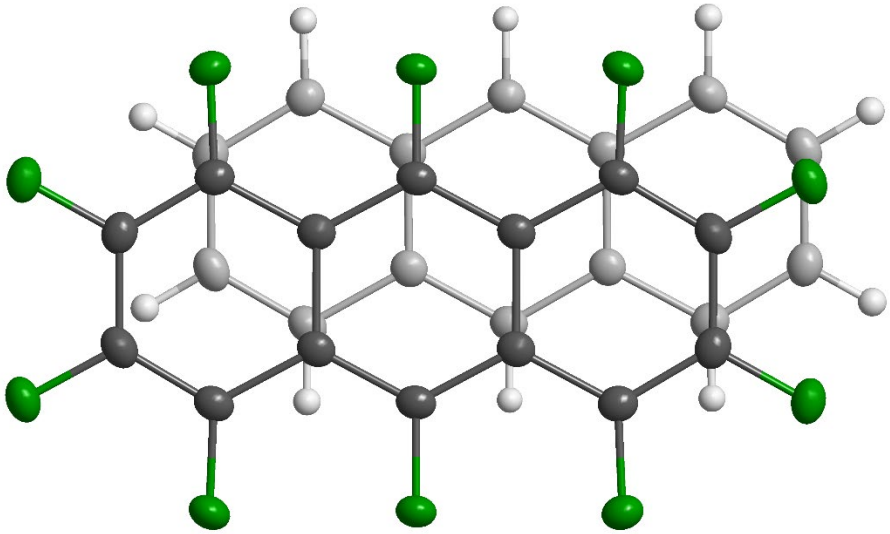

Figure S39. Molecular overlap and π-stacking of decafluoroanthracene with anthracene viewed perpendicular to the decafluoroanthracene mean plane, at 100 K. Fluorine atoms are coloured green in decafluoroanthracene molecules.

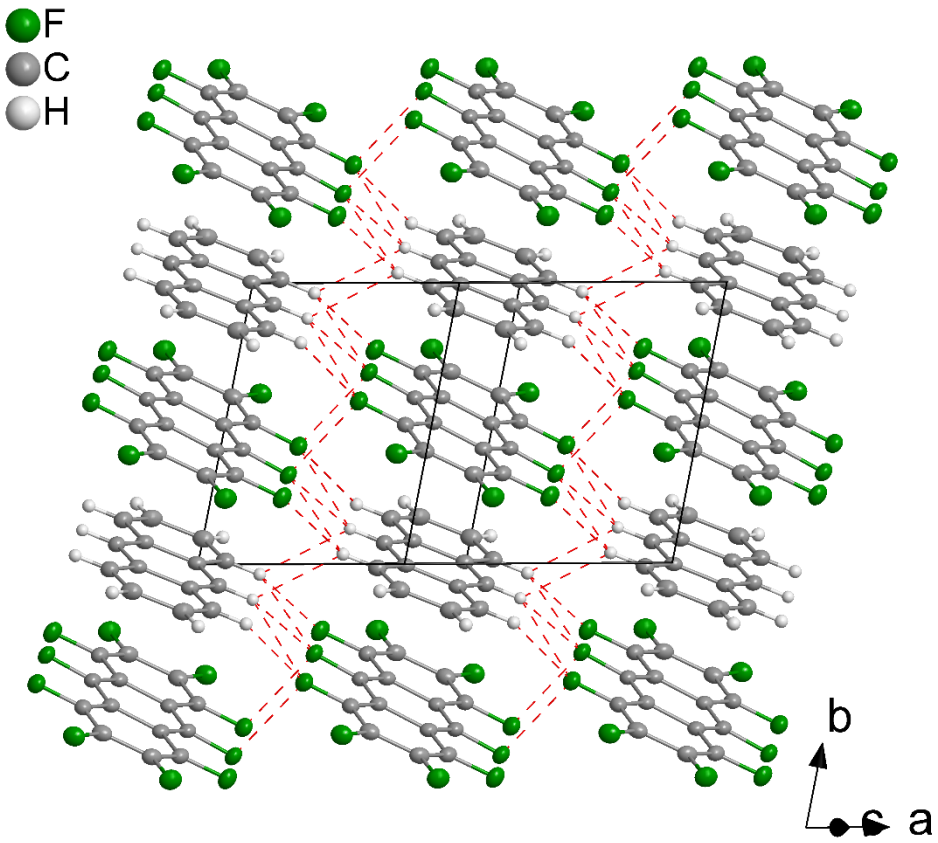

Figure S40. Packing diagram for 1:1 anthracene:decafluoroanthracene (**ADFA**), showing the π-stacking of the components along the *b* axis at 100 K. Intermolecular H···F and F···F contacts between the stacks below the sum of the van der Waals radii are shown as red dashed lines.

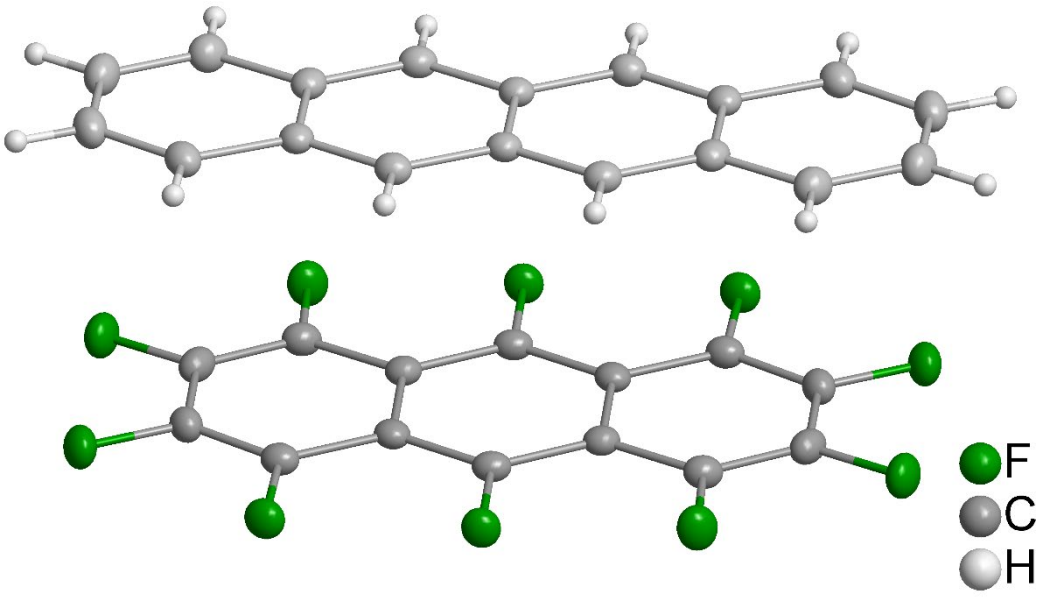

Figure S41. The solid-state molecular structure of 1:1 tetracene:decafluoroanthracene, **TetDFA**, determined by single-crystal X-ray diffraction at 100 K. All ellipsoids are drawn at the 50% probability level. Both molecules have inversion symmetry.

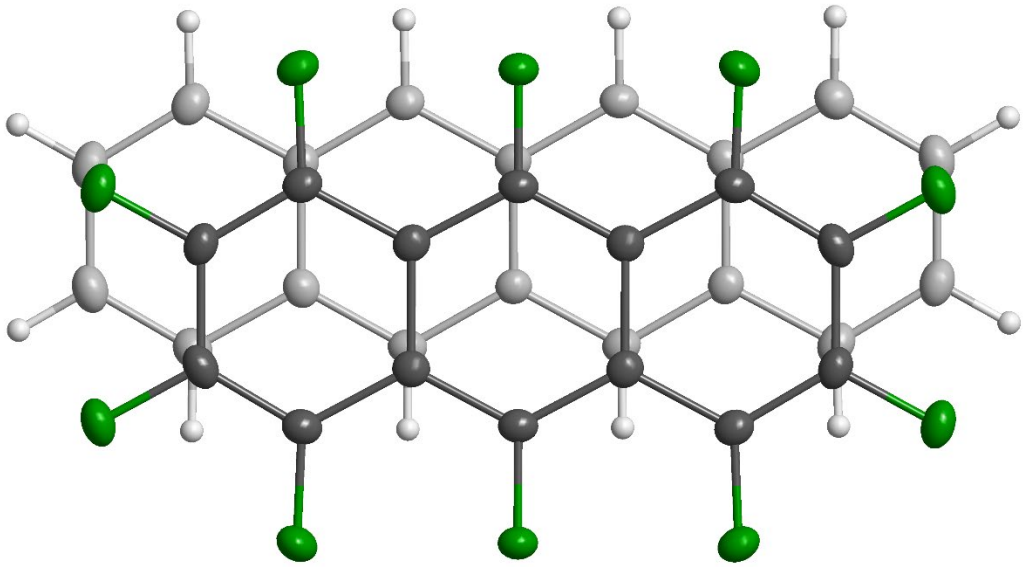

Figure S42. Molecular overlap and π-stacking of decafluoroanthracene with tetracene viewed perpendicular to the decafluoroanthracene mean plane, at 100 K. Fluorine atoms are coloured green in decafluoroanthracene molecules.

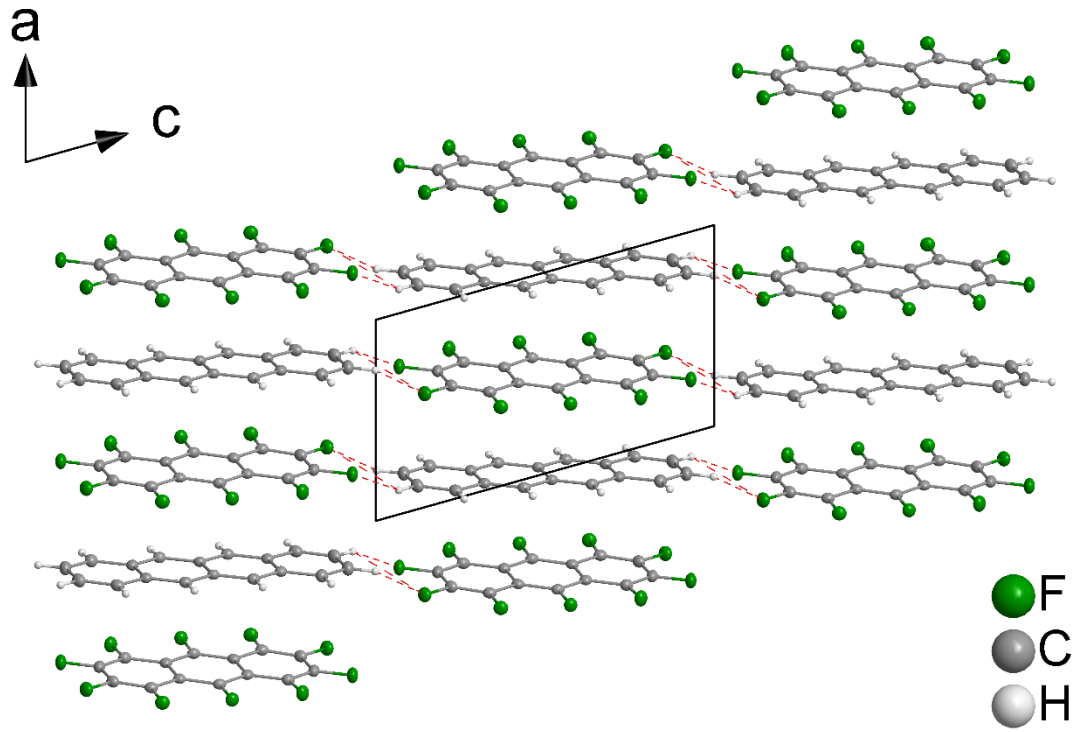

Figure S43. Packing diagram for 1:1 tetracene:decafluoroanthracene (**TetDFA**), showing the π-stacking of the components along the *a* axis at 100 K. Intermolecular H···F contacts between the stacks below the sum of the van der Waals radii are shown as red dashed lines.

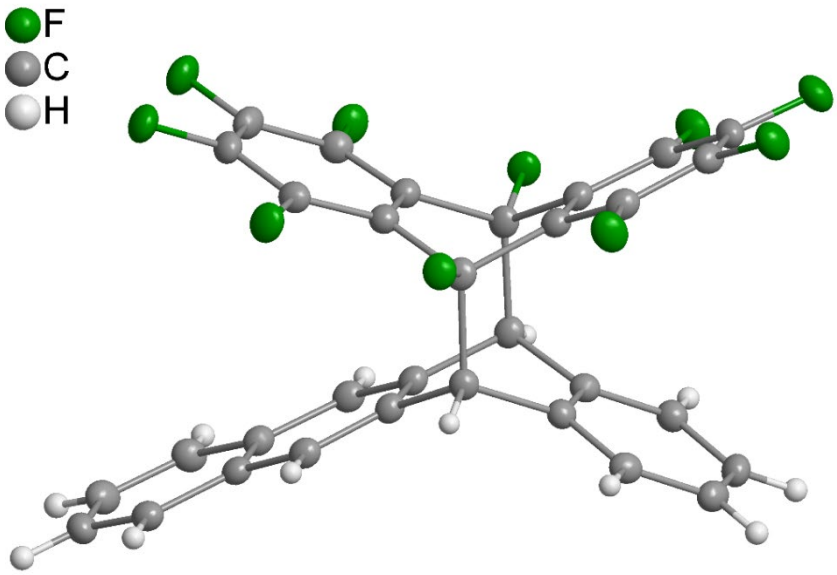

Figure S44. The solid-state molecular structure of tetracene-decafluoroanthracene dimer (**TetDFA-Dimer**) determined by single-crystal X-ray diffraction at 100 K. All ellipsoids are drawn at the 50% probability level.

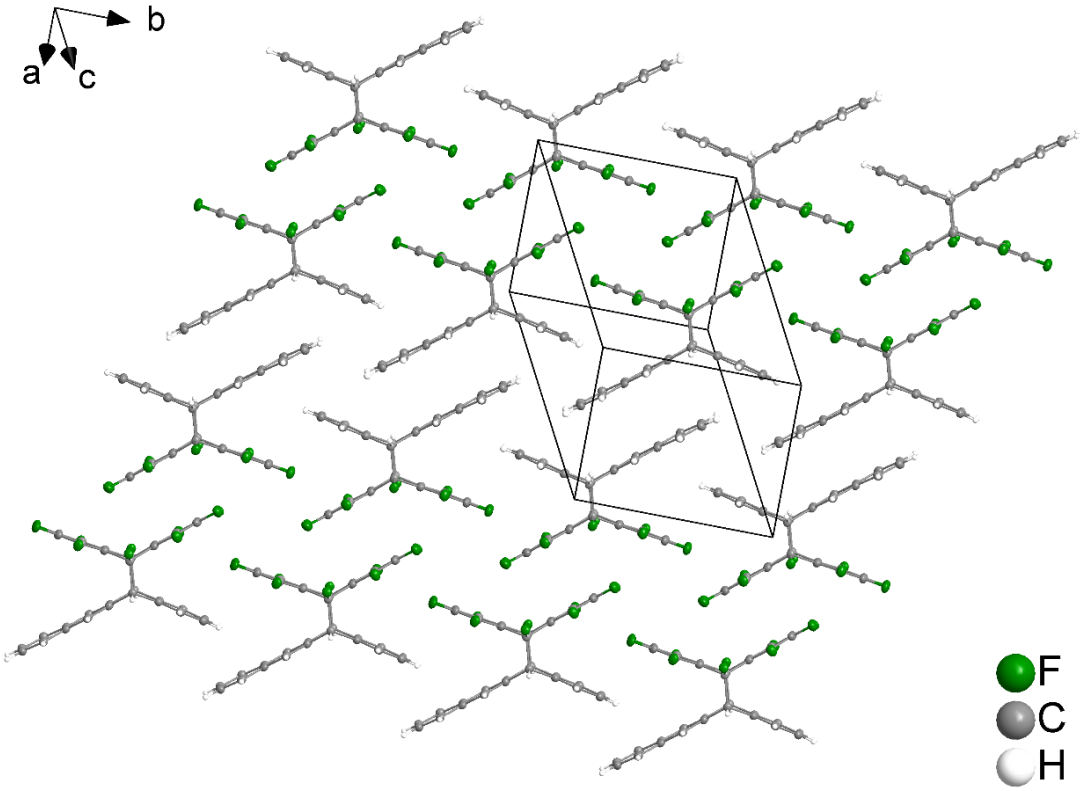

Figure S45. Packing diagram for the tetracene-decafluoroanthracene dimer (**TetDFA-Dimer**), showing the π-stacking between dimers at 100 K. The projection of one sheet is shown here.

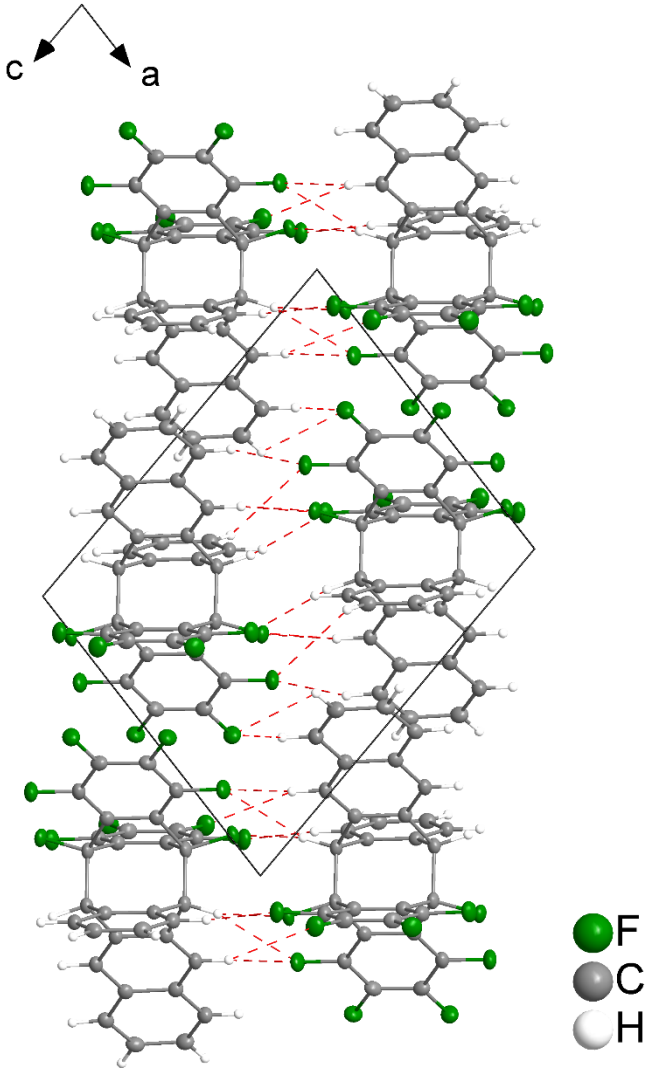

Figure S46. Packing diagram for the tetracene-decafluoroanthracene dimer (**TetDFA-Dimer**), showing the intermolecular H···F contacts between sheets of dimers with distances below the sum of the van der Waals radii as red dashed lines (100 K).

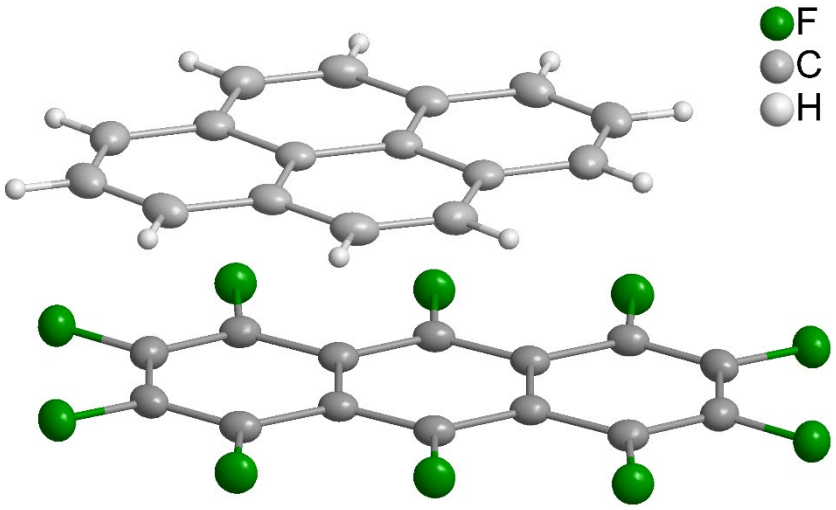

Figure S47. The solid-state molecular structure of 1:1 pyrene:decafluoroanthracene, **PyrDFA**, determined by single-crystal X-ray diffraction at 100 K. All ellipsoids are drawn at the 50% probability level. Both molecules have inversion symmetry.

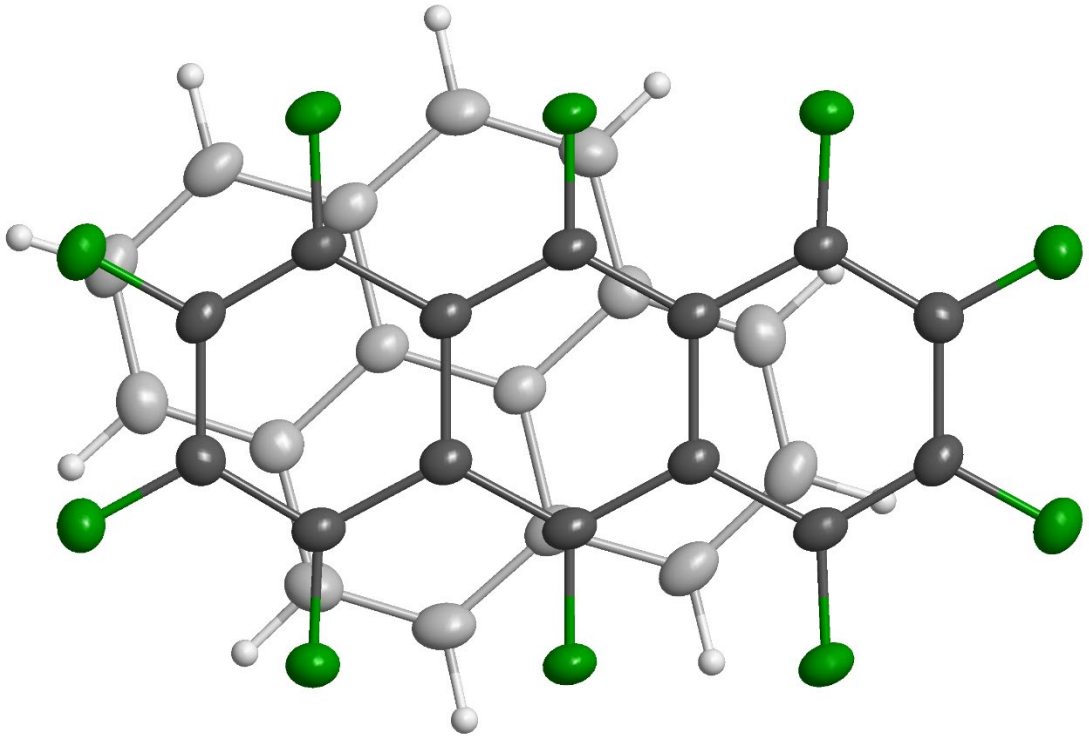

Figure S48. Molecular overlap and π-stacking of decafluoroanthracene with pyrene viewed perpendicular to the decafluoroanthracene mean plane, at 100 K. Fluorine atoms are coloured green in decafluoroanthracene molecules.

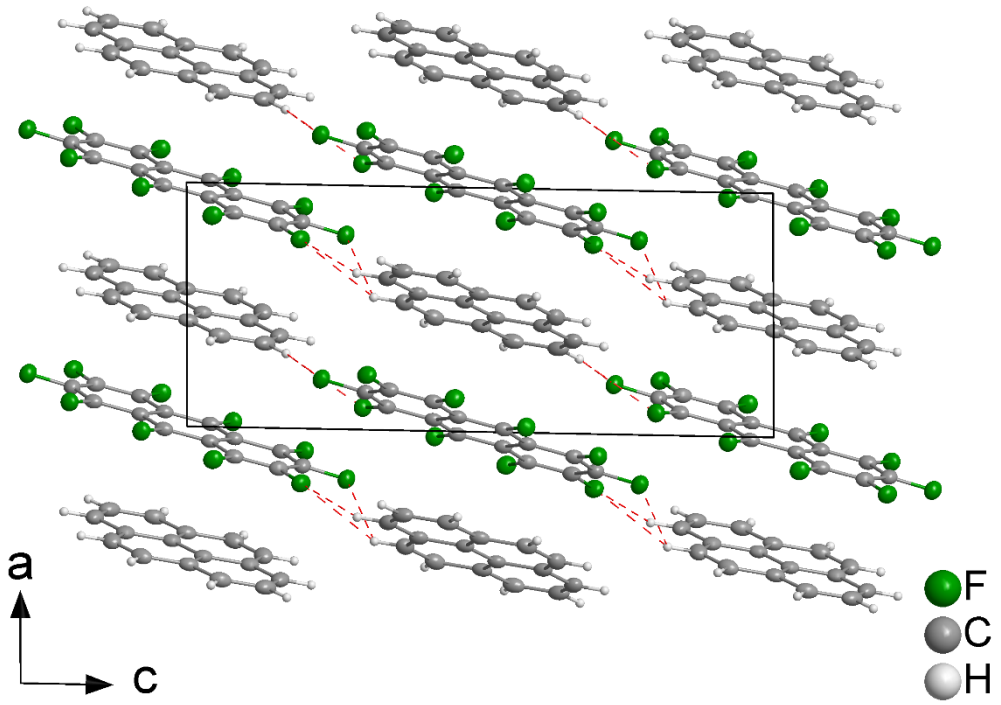

Figure S49. Packing diagram for 1:1 pyrene:decafluoroanthracene (**PyrDFA**), showing the π-stacking of the components at 100 K. Intermolecular H···F contacts between the stacks below the sum of the van der Waals radii are shown as red dashed lines.

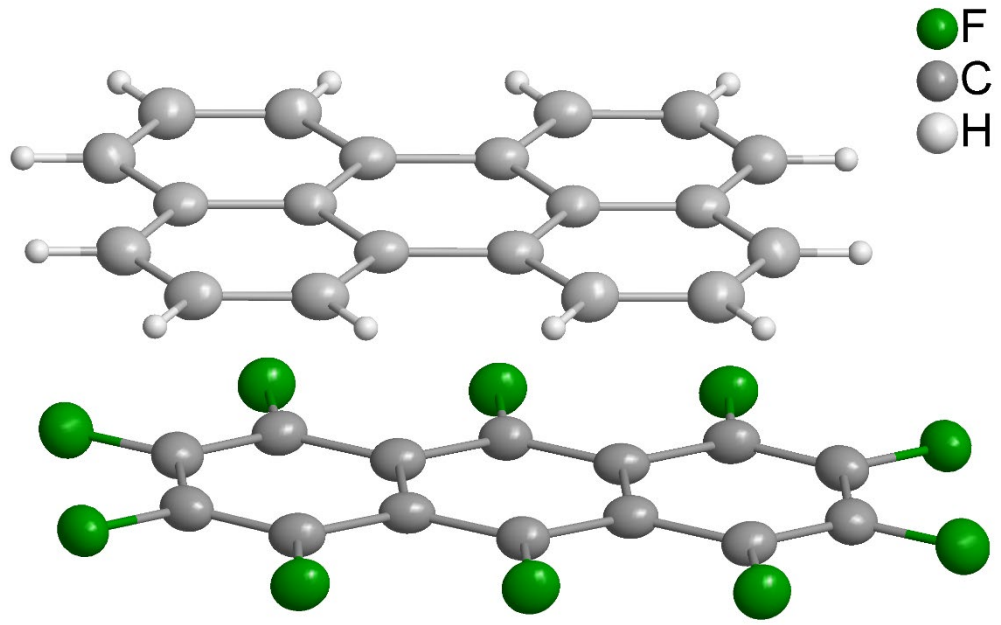

Figure S50. The solid-state molecular structure of 1:1 perylene:decafluoroanthracene, **PerDFA**, determined by single-crystal X-ray diffraction at 100 K. All ellipsoids are drawn at the 50% probability level. Both molecules have inversion symmetry.

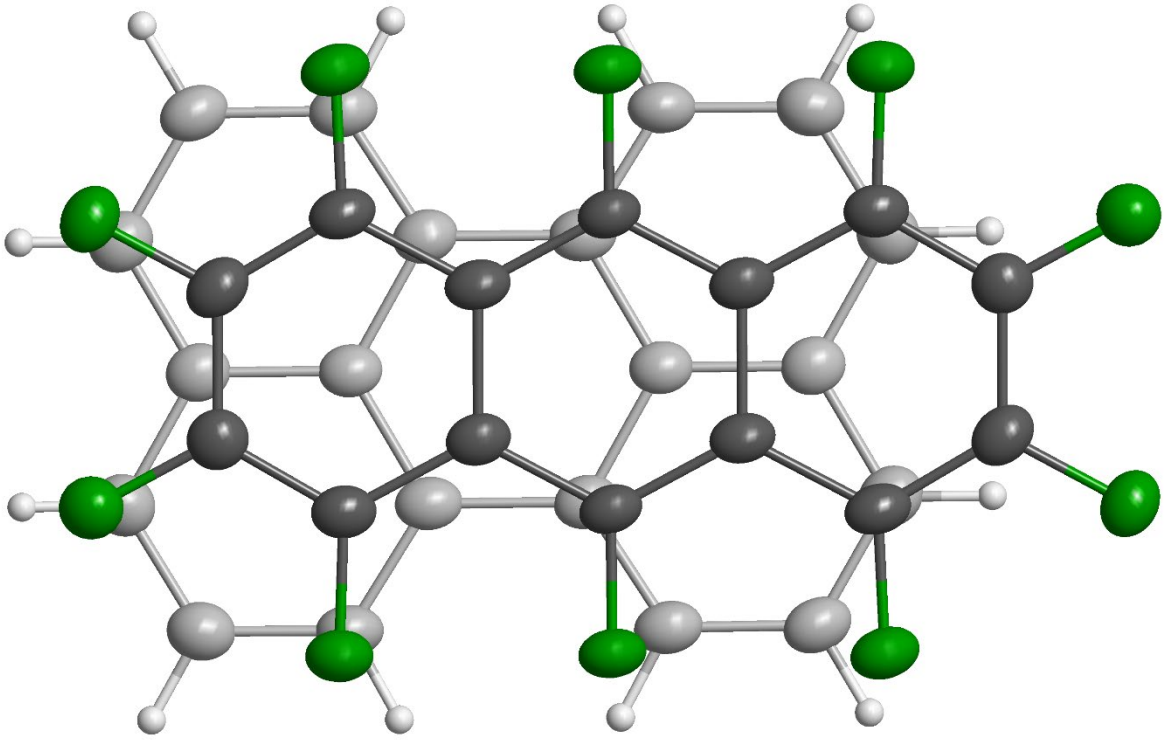

Figure S51. Molecular overlap and π-stacking of decafluoroanthracene with perylene viewed perpendicular to the decafluoroanthracene mean plane, at 100 K. Fluorine atoms are coloured green in decafluoroanthracene molecules.

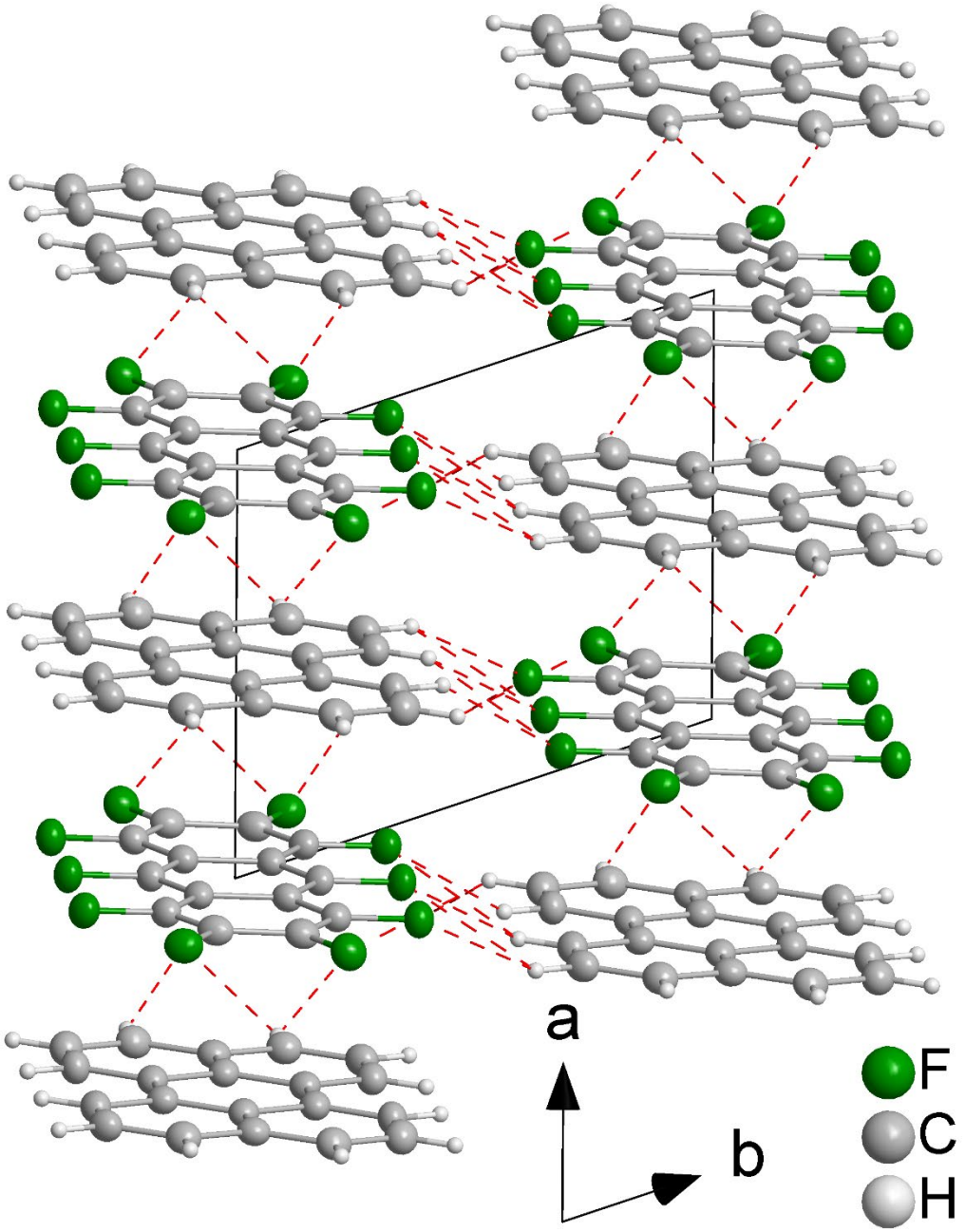

Figure S52. Packing diagram for 1:1 perylene:decafluoroanthracene (**PerDFA**) projected along the *c* axis and showing the π-stacking of the components at 100 K. Intermolecular H···F contacts between the stacks with distances below the sum of the van der Waals radii are shown as red dashed lines.

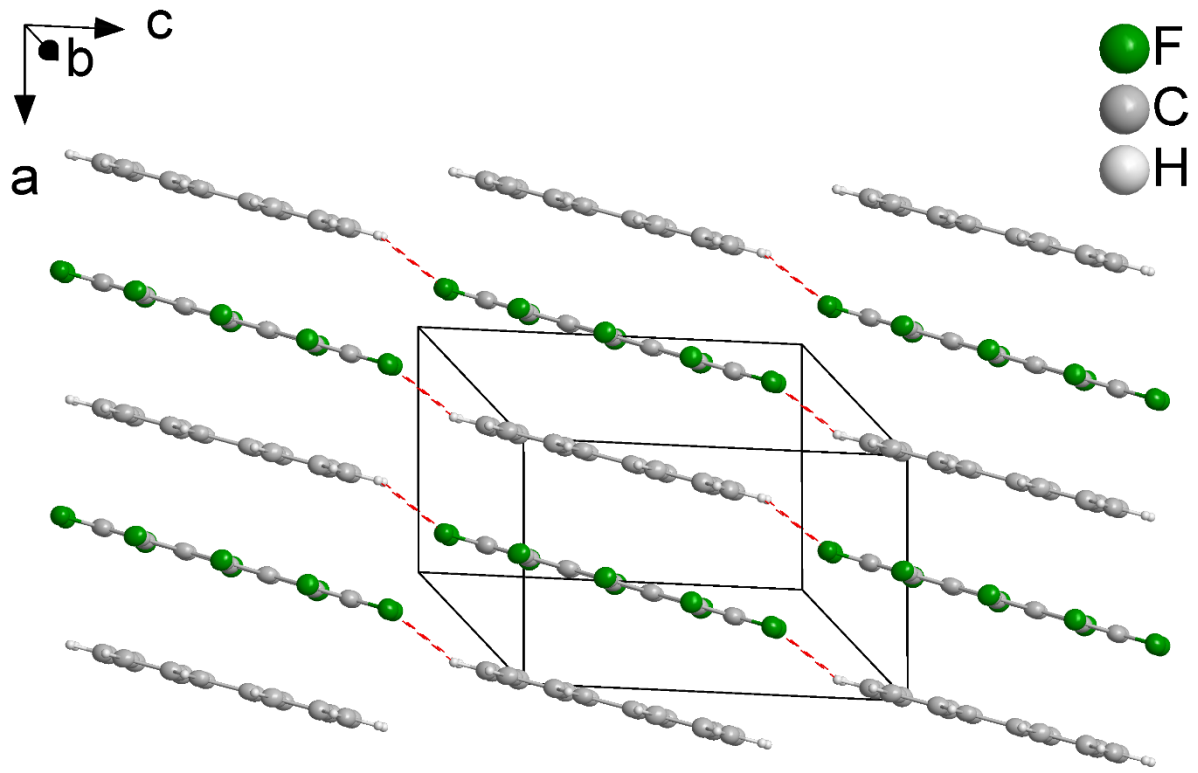

Figure S53. Packing diagram for 1:1 perylene:decafluoroanthracene (**PerDFA**), showing the π-stacking of the components at 100 K. Intermolecular H···F contacts between the stacks below the sum of the van der Waals radii are shown as red dashed lines.

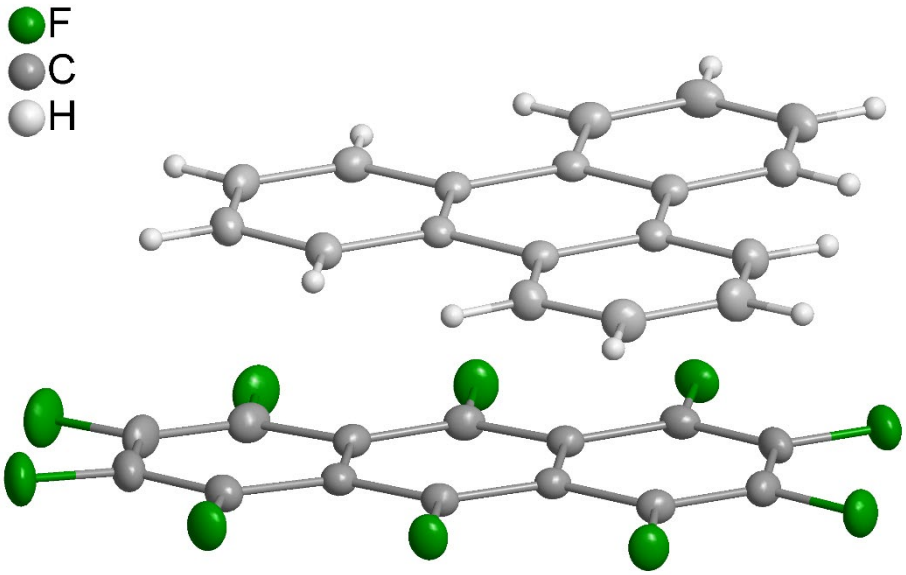

Figure S54. The solid-state molecular structure of 1:1 triphenylene:decafluoroanthracene, **TriDFA**, determined by single-crystal X-ray diffraction at 100 K. All ellipsoids are drawn at the 50% probability level.

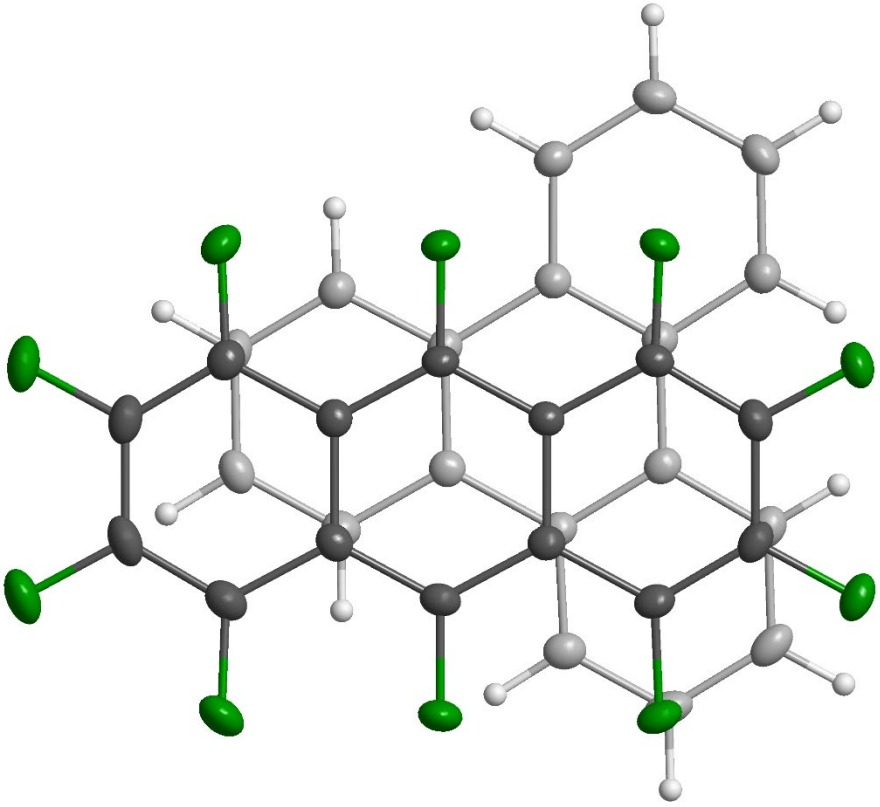

Figure S55. Molecular overlap and π-stacking of decafluoroanthracene with triphenylene viewed perpendicular to the decafluoroanthracene mean plane, at 100 K.

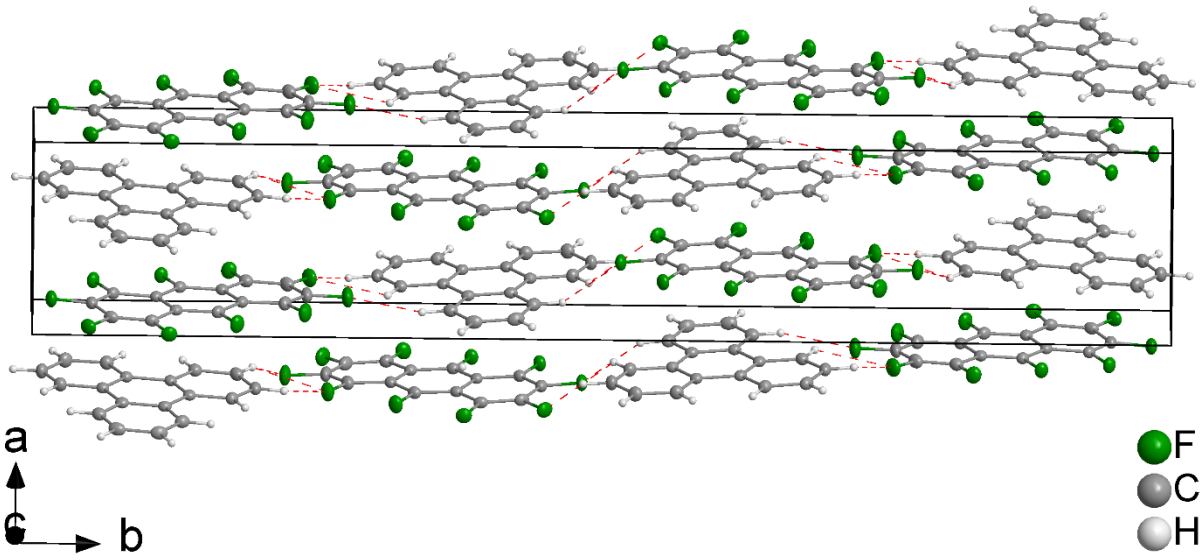

Figure S56. Packing diagram for 1:1 triphenylene:decafluoroanthracene, showing the π-stacking of the components at 100 K. Intermolecular H···F contacts between the stacks with distances below the sum of the van der Waals radii are shown as red dashed lines.

Table S3. C–C bond distances (Å) of the **ADFA** co-crystal and pure **DFA** at 100 K and 299 K, respectively. The anthracene (**A**) and **DFA** molecules all have inversion symmetry.

	ADFA		**DFA**
	100 K	299 K	100 K
A-R1			**DFA-R1 (molecule 1)**
C1–C2	1.3618(17)	1.349(4)	1.347(3)
C2–C3	1.4242(18)	1.416(5)	1.419(3)
C3–C4	1.3649(17)	1.343(4)	1.352(3)
C4–C5	1.4299(17)	1.422(4)	1.420(3)
C5–C7	1.4404(17)	1.440(4)	1.448(3)
C7–C1	1.4324(16)	1.418(4)	1.430(3)
A-R2			**DFA-R2 (molecule 1)**
C5–C6	1.3977(16)	1.393(4)	1.399(3)
C6–C7	1.4008(17)	1.389(4)	1.381(3)
DFA-R1			**DFA-R1 (molecule 2)**
C8–C9	1.3531(18)	1.358(4)	1.351(3)
C9–C10	1.4120(17)	1.409(4)	1.421(3)
C10–C11	1.3556(17)	1.332(4)	1.353(3)
C11–C12	1.4234(17)	1.417(4)	1.422(3)
C12–C14	1.4440(17)	1.449(4)	1.448(3)
C14–C8	1.4279(16)	1.407(4)	1.427(3)
DFA-R2			**DFA-R2 (molecule 2)**
C12–C13	1.3958(17)	1.389(4)	1.392(3)
C13–C14	1.3927(18)	1.386(4)	1.392(3)

Table S4. C–C bond distances (Å) of **TetDFA-Dimer** and the **TetDFA** co-crystal at 100 K and 298 K, respectively.

	TetDFA-Dimer			**TetDFA**	
	100 K	298 K		100 K	298 K
DFA-R1			**DFA-R1/R3**		
C3–C4	1.3835(19)	1.380(2)	C1–C2	1.3544(19)	1.347(2)
C4–C5	1.3730(19)	1.368(2)	C2–C3	1.408(2)	1.400(2)
C5–C6	1.3875(18)	1.3811(19)	C3–C4	1.3523(19)	1.347(2)
C6–C7	1.3866(18)	1.3809(18)	C4–C5	1.4248(18)	1.4245(19)
C7–C2	1.4034(17)	1.4033(16)	C5–C7	1.4432(19)	1.4375(19)
C2–C3	1.3845(17)	1.3800(17)	C7–C1	1.4223(19)	1.422(2)
DFA-R3					
C9–C10	1.3841(18)	1.3832(17)			
C10–C11	1.3852(18)	1.3812(19)			
C11–C12	1.3741(19)	1.368(2)			
C12–C13	1.3850(18)	1.3801(19)			
C13–C14	1.3889(18)	1.3839(18)			
C14–C9	1.4023(17)	1.4005(16)			
DFA-R2			**DFA-R2**		
C1–C2	1.5212(17)	1.5186(17)	C5–C6	1.3919(19)	1.3892(19)
C7–C8	1.5209(17)	1.5217(16)	C6–C7	1.3940(19)	1.3914(19)
C8–C9	1.5222(17)	1.5195(17)			
C14–C1	1.5239(17)	1.5240(16)			
Interconnecting bonds					
C1–C15	1.5985(17)	1.5935(17)			
C8–C26	1.5966(17)	1.5895(17)			
Tet-R2					
C15–C16	1.5180(17)	1.5187(16)			
C32–C15	1.5113(17)	1.5147(16)			
C25–C26	1.5159(17)	1.5153(16)			
C26–C27	1.5216(17)	1.5195(16)			
Tet-R1			**Tet-R1/R4**		
C28–C29	1.3929(18)	1.3896(19)	C8–C9	1.3644(19)	1.353(2)
C29–C30	1.3897(18)	1.381(2)	C9–C10	1.428(2)	1.408(3)
C30–C31	1.3916(18)	1.3860(19)	C10–C11	1.355(2)	1.353(2)
C31–C32	1.3882(17)	1.3835(17)	C11–C12	1.4396(18)	1.4338(19)
C32–C27	1.4005(17)	1.3999(16)	C12–C16	1.4431(19)	1.438(2)
C27–C28	1.3888(17)	1.3859(17)	C16–C8	1.4321(18)	1.429(2)
Tet-R3			**Tet-R2/R3**		
C16–C17	1.3673(17)	1.3651(16)	C12–C13	1.3870(19)	1.3839(19)
C17–C18	1.4234(18)	1.4227(18)	C13–C14	1.4139(19)	1.4098(18)
C23–C24	1.4230(18)	1.4200(18)	C14–C15	1.4057(19)	1.4054(19)
C24–C25	1.3687(18)	1.3650(17)	C15–C16	1.3944(19)	1.3884(19)
C25–C16	1.4258(17)	1.4224(15)	C14–C14	1.443(2)	1.438(2)
Tet-R4					
C18–C19	1.4195(17)	1.4166(17)			
C19–C20	1.3702(19)	1.365(2)			
C20–C21	1.4095(19)	1.399(2)			
C21–C22	1.3708(19	1.365(2)			
C22–C23	1.4200(18)	1.4169(19)			
C23–C18	1.4221(18)	1.4183(17)			

Table S5. Aryl···aryl (π···π) distances (Å) in crystals of **NDFA**, **ADFA**, **TetDFA**, **TetDFA-Dimer**, **PyrDFA**, **PerDFA**, and **TriDFA** at 100 K: centroid-centroid distance, interplanar separation, and offset shift.

Compound	Aryl···Aryl	Centroid-centroid distance	Interplanar separation	Offset shift [a]
NDFA	Aryl(F)···Aryl(H)	3.7048(1)	3.4330(17) 3.3767(16)	1.393(4) 1.524(4)
ADFA	Aryl(F)···Aryl(H)	3.67115(10)	3.4495(4) 3.3480(5)	1.2564(10) 1.5062(11)
TetDFA	Aryl(F)···Aryl(H)	3.45575(10)	3.3827(3) 3.3209(5)	0.7067(15) 0.9559(17)
TetDFA-Dimer	Naph(H)···Naph(H)	3.7758(10)	3.5044(12)	1.4056(19)
	Benz(F)···Benz(F)	3.7644(13)	3.5399(16)	1.281(3)
	Naph(H) ···Benz(F) intra	4.2464(8)	3.3999(11) 4.2464(8)	2.6216(12) 0.632(3) Tilt: 46.02(4)°
	Benz(H) ···Benz(F) intra	3.8096(9)	3.3889(12) 3.4663(14)	1.740(2) 1.581(2) Tilt: 46.7(4)°
PyrDFA	Aryl(F)···Aryl(H)	3.57765(10)	3.3733(3) 3.3814(3)	1.1917(8) 1.1687(8)
PerDFA	Aryl(F)···Aryl(H)	3.4846(3)	3.3639(4) 3.3458(4)	0.9090(11) 0.9737(12)
TriDFA	Aryl(F)···Aryl(H)	3.7059(4) 3.8475(4)	3.3504(5) 3.3653(5) 3.3412(5) 3.3583(5)	1.5838(8) 1.5518(6) 1.9078(6) 1.8775(7)

[a] The offset shift, also called inter-centroid shift, is the distance within a plane of an aryl ring between the centroid of the respective aryl ring and the intersection point with the normal to the plane through the centroid of the other aryl ring.

Table S6. Intermolecular distances (Å) and molecular slip angles (°) of the 1:1 co-crystals of aryl (**N** = naphthalene, **A** = anthracene, **Tet** = tetracene, **Pyr** = pyrene, **Per** = perylene, **Tri** = triphenylene) with decafluoroanthracene, **DFA**, $C_{14}F_{10}$ at 100 K.

Compound	Repeat centroid-centroid dist.	**DFA** interplanar separation	**Aryl** interplanar separation	Intercomponent centroid-centroid distance	Mean intercomponent interplanar sep.	**DFA** slip angle	**Aryl** slip angle
NDFA	7.4096(2)	6.753(3)	6.866(4)	3.7048(1)	3.4330(17) 3.3767(16)	24.3	22.1
ADFA	7.3423(2)	6.6959(10)	6.8989(8)	3.67115(10)	3.4495(4) 3.3480(5)	24.2	20.0
TetDFA	6.9115(2)	6.6419(10)	6.7654(7)	3.45575(10)	3.3827(3) 3.3209(5)	16.0	11.8
PyrDFA	7.1553(2)	6.7467(6)	6.7628(6)	3.57765(10)	3.3733(3) 3.3814(3)	19.4	19.1
PerDFA	6.9692(5)	6.6916(8)	6.7279(7)	3.4846(3)	3.3639(4) 3.3458(4)	16.2	15.1
TriDFA	6.71719(9)	6.7087(1)	6.7065(1)	3.7059(4) 3.8475(4)	3.3504(5) 3.3653(5) 3.3412(5) 3.3583(5)	2.9	3.2

Table S7. Intermolecular C–H···F, H···F, H···H, C···F, C···C, and F···F interaction distances (Å) in compounds **DFA**, **NDFA**, **ADFA**, **TetDFA**, **TetDFA-Dimer**, **PyrDFA**, **PerDFA**, and **TriDFA** at 100 K less than or equal to the sum of the Van der Waals radii.

Compound	Contact	H···F/H	C/F···C/F
DFA	F3···F8		2.765
	F2···F7		2.824
	F3···F7		2.919
	C1···F5		3.079
	C13···F9		3.091
	C2···F4		3.139
	C11···F10		3.145
	C7···F5		3.153
	C6···F1		3.154
	C8···F9		3.159
	C14···F9		3.163
	C1···C4		3.227
	C6···C6		3.253
	C8···C11		3.255
	C13···C13		3.263
NDFA	C4–H4···F5	2.445	3.132
	H4···F4	2.584	
	H3···F2	2.617	
	F4···F5		2.842
	F3···C7		3.050
	C2···C6		3.316
ADFA	H6···F5	2.587	
	H1···F4	2.591	
	H4···F5	2.618	
	H2···F3	2.635	
	H6···F4	2.653	
	H4···F1	2.654	
	C8···C7		3.303
	C13···C5		3.308
	C11···C3		3.385
	C10···C4		3.395
	C10···F3		3.138
	F4···F5		2.768
	F3···F3		2.771
TetDFA	H15···F4	2.497	
	H13···F5	2.544	
	H11···F1	2.622	
	H8···F2	2.638	
	H11···F5	2.664	
	F4···F5		2.792
	C6···C14		3.269
	C4···C12		3.271
	C1···C16		3.306

Table S7. continued.

Compound	Contact	H···F/H	C/F···C/F
TetDFA-Dimer	H31···H31	2.328	
	H28···F6	2.370	
	H17···F1	2.493	
	H15···F2	2.565	
	H24···F7	2.572	
	H26···F7	2.636	
	H17···F2	2.642	
	C12···F3		2.863
	C11···F3		2.931
	C2···F8		3.109
PyrDFA	H3···F4	2.523	
	H2···F2	2.570	
	H1···F3	2.648	
	F1···F3		2.882
	F4···F4		2.916
	C11···F1		3.150
	C9···C6		3.308
	C14···C4		3.324
	C10···C7		3.397
PerDFA	H15···F4	2.537	
	H14···F1	2.565	
	H13···F5	2.579	
	H10···F3	2.655	
	C1···C12		3.347
	C4···C16		3.355
	C5···C8		3.385
	C4···C8		3.387
	C7···C12		3.394
TriDFA	H3···F5	2.580	
	H14···F1	2.617	
	H9···F4	2.618	
	H3···F6	2.622	
	H5···F3	2.631	
	H16···F7	2.639	
	H15···F9	2.646	
	F7···F9		2.866
	F3···F3		2.935
	C27···F9		3.137
	C15···C26		3.260
	C13···C24		3.302
	C5···C20		3.339
	C7···C22		3.367
	C1···C32		3.386
	C17···C30		3.397

Table S8. Intermolecular H···F, C···F, C···C, and F···F interaction distances (Å) in compounds **NDFA**, **ADFA**, **TetDFA**, **PyrDFA**, and **TriDFA** at ambient temperature less than or equal to the sum of the Van der Waals radii.

Compound	Contact	H···F/H	C/F···C/F
NDFA	H4···F5	2.534	
	F4···F5		2.927
	F3···C7		3.164
	C2···C6		3.381
ADFA	F4···F5		2.853
	F3···F3		2.863
	C13···C5		3.384
	C8···C7		3.390
TetDFA	F4···F5		2.860
	C6···C14		3.336
	C4···C12		3.338
	C1···C16		3.371
	H15···F4	2.576	
	H13···F5	2.638	
PyrDFA	H3···F4	2.668	
	H1···F3	2.639	
	C9···C6		3.392
	C14···C4		3.399
TriDFA	C15···C26		3.320
	C13···C24		3.373

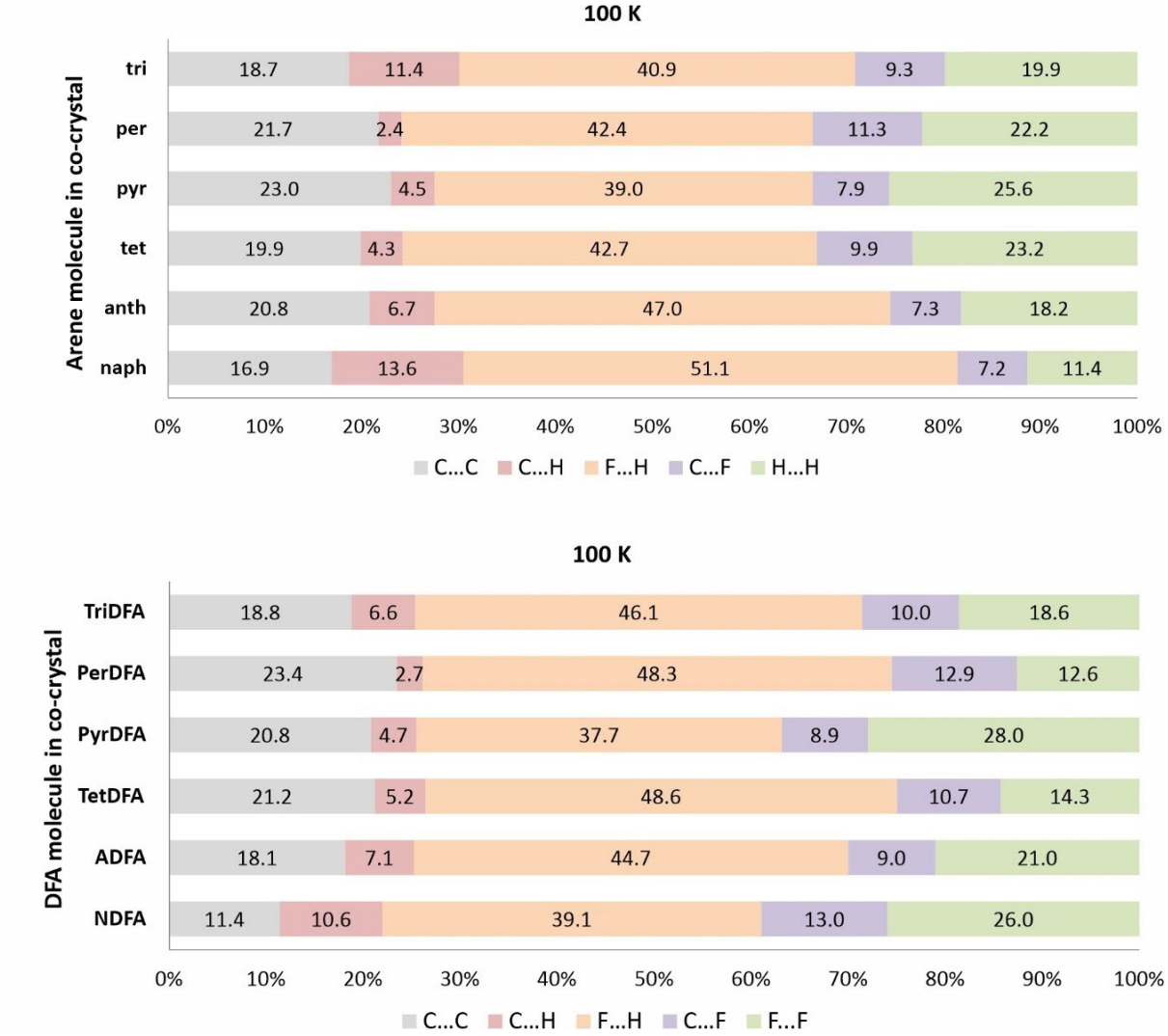

Figure S57. Percentage contributions to the Hirshfeld surface area for the various close intermolecular contacts in the individual molecules of the co-crystals **NDFA**, **ADFA**, **TetDFA**, **PyrDFA**, **PerDFA**, and **TriDFA** at 100 K.

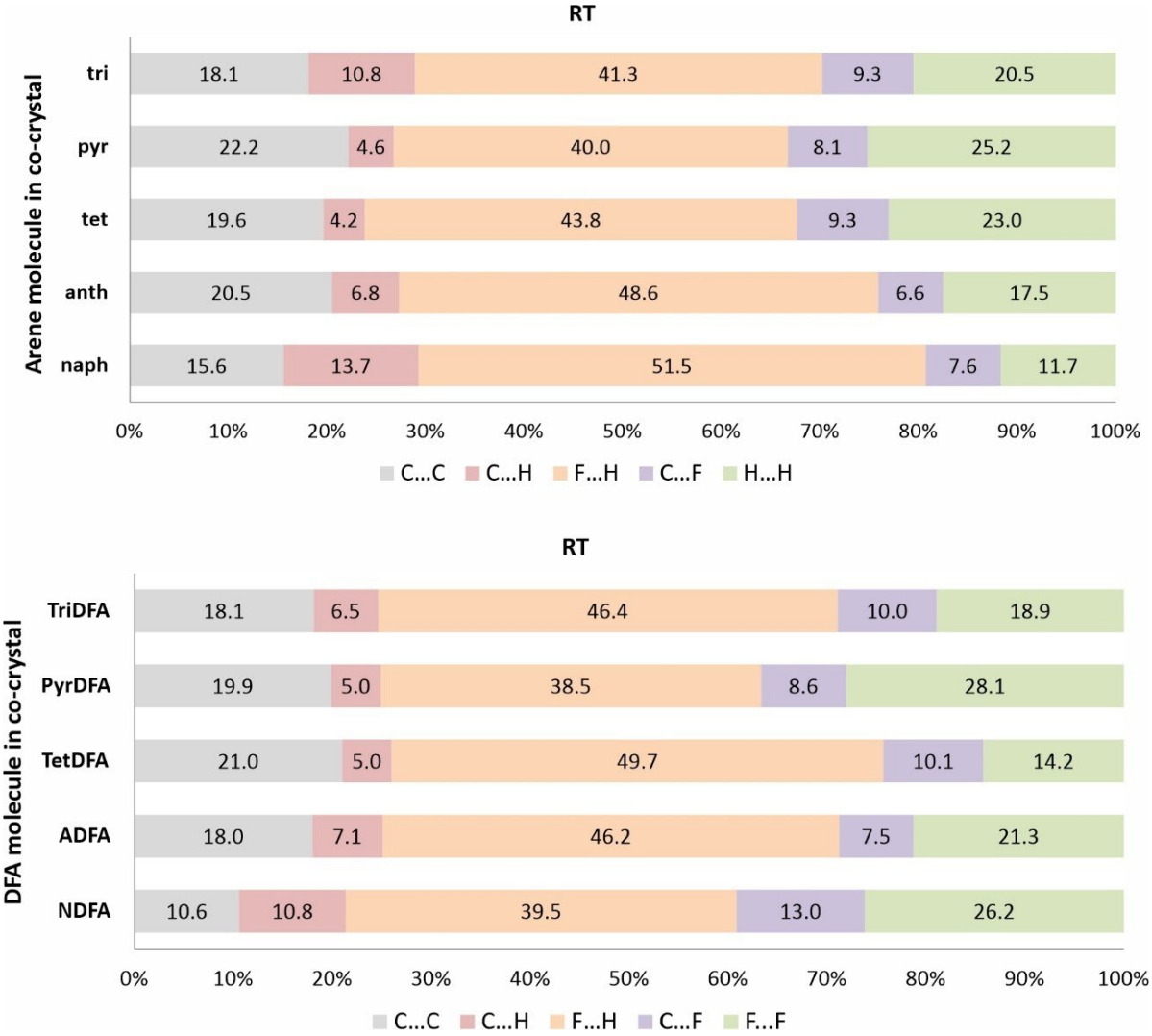

Figure S58. Percentage contributions to the Hirshfeld surface area for the various close intermolecular contacts in the individual molecules of the co-crystals **NDFA**, **ADFA**, **TetDFA**, **PyrDFA**, **PerDFA**, and **TriDFA** at room temperature.

Table S9. Properties of the individual molecules in the co-crystals of compounds **NDFA**, **ADFA**, **TetDFA**, **PyrDFA**, and **TriDFA** at RT: volume within van der Waals (V_m), Hirshfeld volume (V_H), and surface volume of the crystal voids (V_v), crystal packing coefficient (c_k), and percentage of intermolecular contacts.

	N/DFA	**A/DFA**	**Tet/DFA**	**Pyr/DFA**	**Tri/DFA**
V_m / Å³	115.7/216.7	157.1/216.6	198.5/216.7	172.8/216.3	198.3/217.1
V_H / Å³	176.2/289.4	237.64/282.4	299.4/277.7	257.7/283.3	292.5/290.3
V_V / Å³	118.01 (59.0)[a]	62.1	69.9	135.2 (67.6)[a]	306.9 (76.7)[a]
c_k	0.70	0.71	0.71	0.71	0.70
C···C / %	15.6/10.6	20.5/18.0	19.6/21.0	22.2/19.9	18.1/18.1
C···F / %	7.6/13.0	6.6/7.5	9.3/10.1	8.1/8.6	9.3/10.0
C···H / %	13.7/10.8	6.8/7.1	4.2/5.0	4.6/5.0	10.8/6.5
H···H / %	11.7/ -	17.5/ -	23.0/ -	25.2/ -	20.5/ -
F···H / %	51.5/39.5	48.6/46.2	43.8/49.7	40.0/38.5	41.3/46.4
F···F / %	- /26.2	- /21.3	- /14.2	- /28.1	- /18.9

[a] The value in brackets is normalized to a comparable unit-cell volume to **ADFA** and **TetDFA**, i.e., divided by two for **NDFA** and **PyrDFA**, and by four for **TriDFA**.

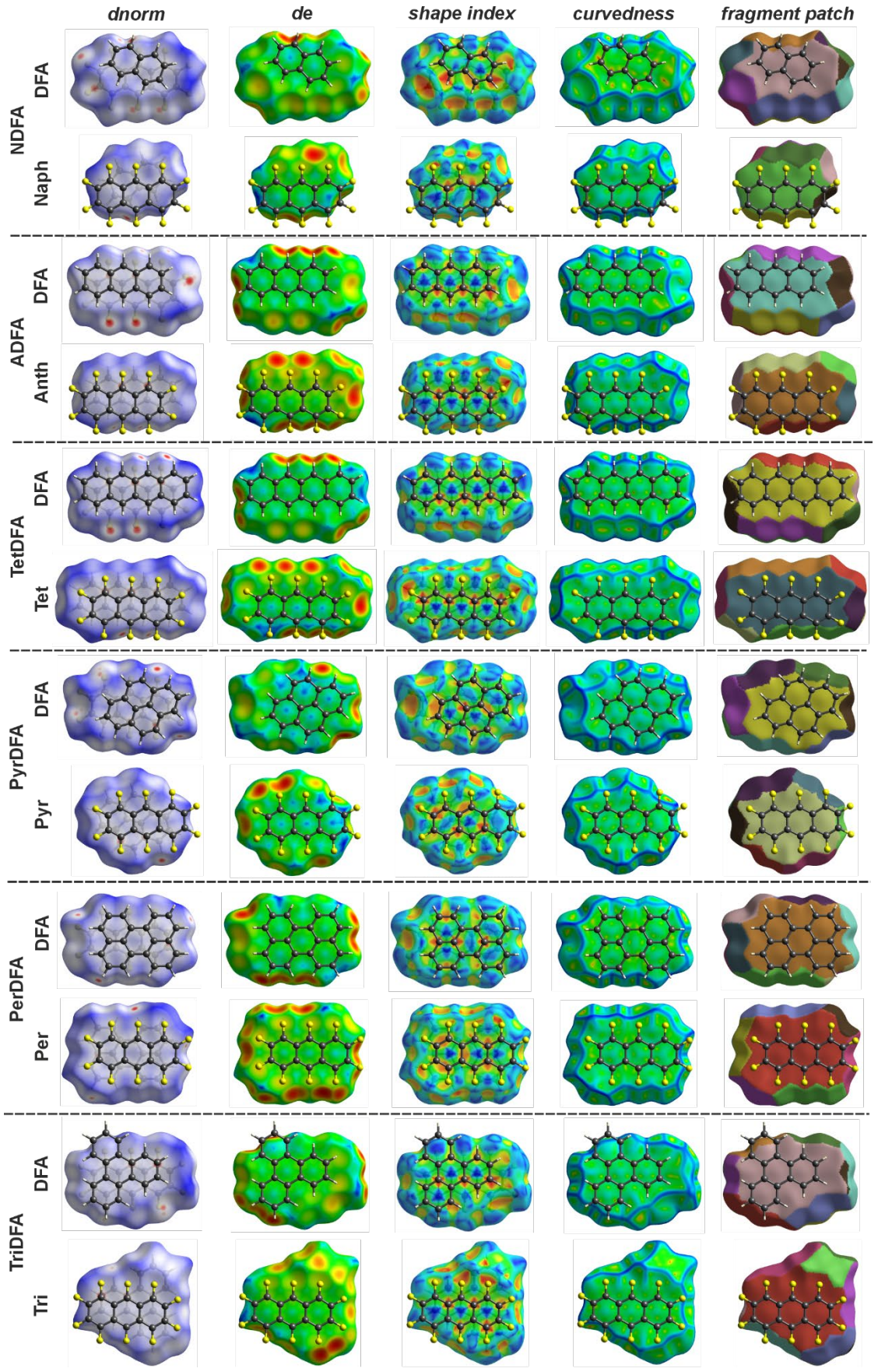

Figure S59. Hirshfeld surfaces of the arene and decafluoroanthracene molecules of the co-crystals at 100 K mapped with d_{norm}, d_e, shape index, curvature, and fragment patch.

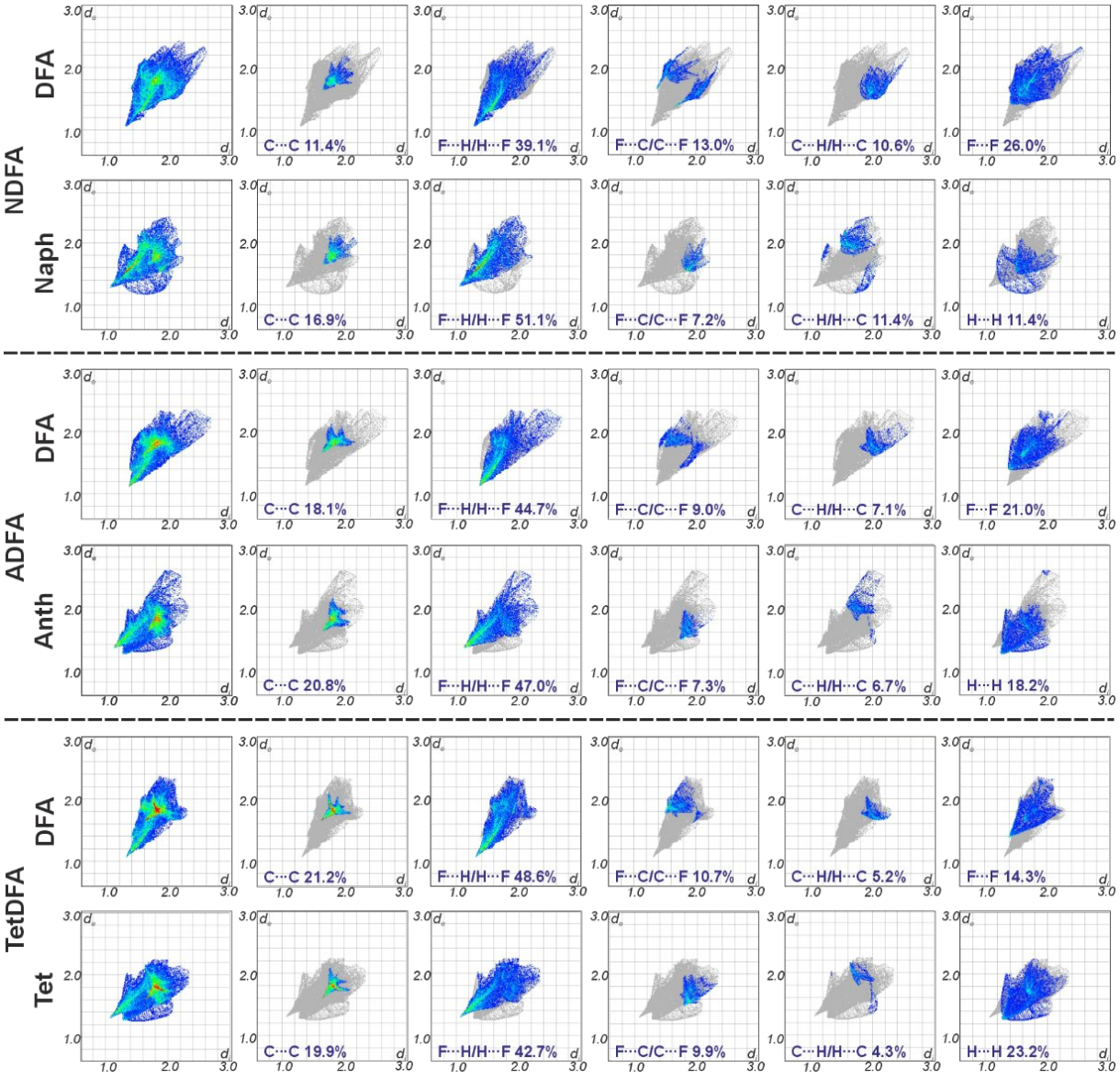

Figure S60. Two-dimensional fingerprint plots of the arene and decafluoroanthracene molecules of the co-crystals **NDFA**, **ADFA** and **TetDFA** calculated from the Hirshfeld surfaces at 100 K. The left column shows the complete fingerprint plots, while the other plots indicate the contributions of the individual intermolecular interactions (C···C, F···H, F···C, C···H, and H···H from left to right) within the grey area of all contributions.

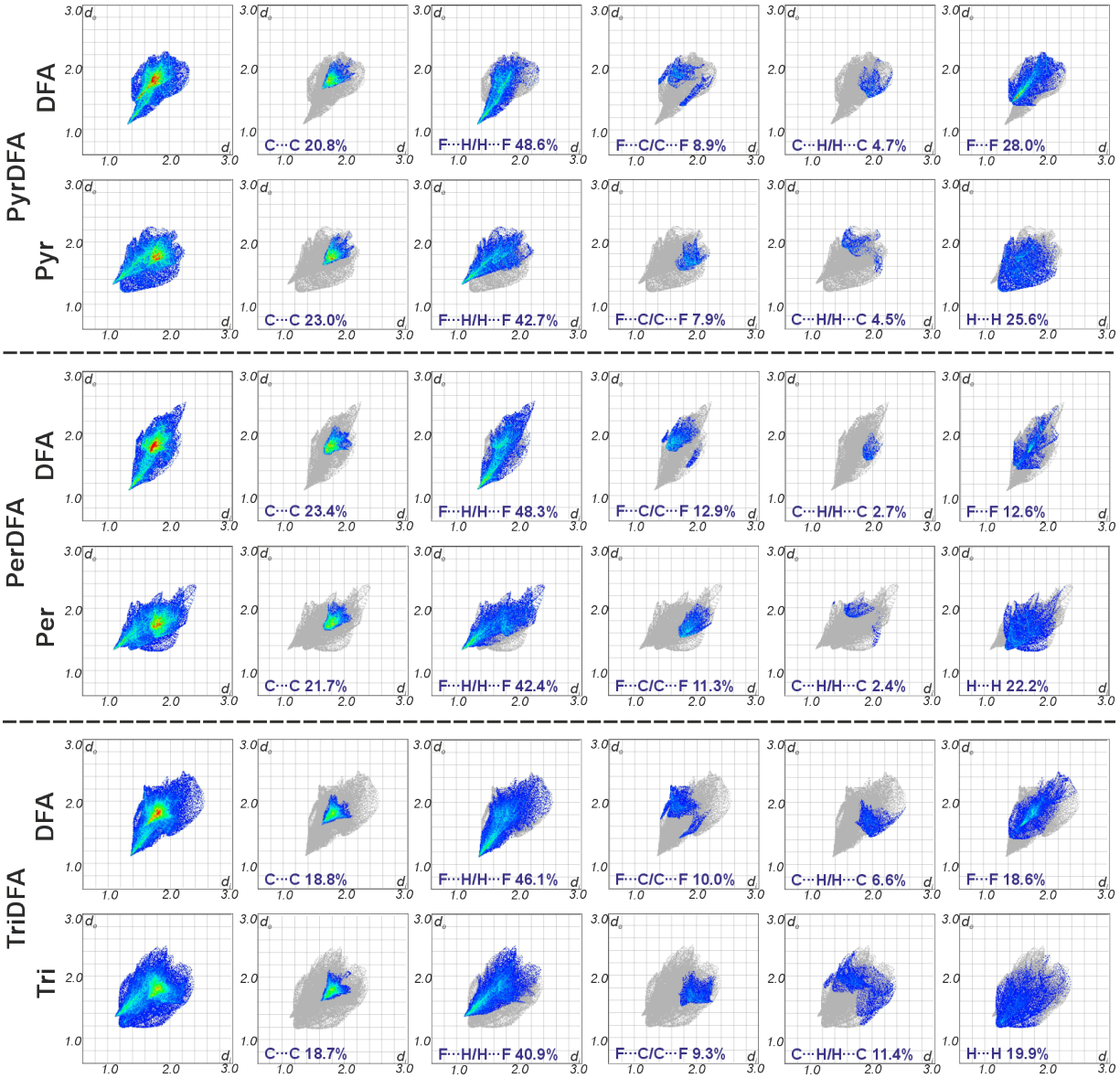

Figure S61. Two-dimensional fingerprint plots of the arene and decafluoroanthracene molecules of the co-crystals **PyrDFA**, Per**DFA** and **TriDFA** calculated from the Hirshfeld surfaces at 100 K. The left column shows the complete fingerprint plots, while the other plots indicate the contributions of the individual intermolecular interactions (C···C, F···H, F···C, C···H, and H···H from left to right) within the grey area of all contributions.

Table S10. Enrichment ratios for the pairs of chemical species of the individual arene and decafluoroanthracene molecules of compounds **NDFA**, **ADFA** and **TetDFA** at 100 K.

NDFA: Naph				
Contact%	Atoms	C	H	F
	C	16.9	1.7	7.2
	H	11.9	11.4	51.1
Surface%		27.3	43.8	29.2
Random Contacts%	Atoms	C	H	F
	C	7.5		
	H	23.9	19.1	
	F	15.9	25.5	8.5
Enrichment Ratio	Atoms	C	H	F
	C	**2.27**		
	H	0.57	0.60	
	F	0.45	**2.00**	0.00
ADFA: Anth				
Contact%	Atoms	C	H	F
	C	20.8	0.3	7.3
	H	6.4	18.2	47
Surface%		27.8	45.1	27.2
Random Contacts%	Atoms	C	H	F
	C	7.7		
	H	25.0	20.3	
	F	15.1	24.5	7.4
Enrichment Ratio	Atoms	C	H	F
	C	**2.69**		
	H	0.27	0.90	
	F	0.48	**1.92**	0.00
TetDFA: Tet				
Contact%	Atoms	C	H	F
	C	19.9	0.5	9.9
	H	3.8	23.2	42.7
Surface%		27	46.7	26.3
Random Contacts%	Atoms	C	H	F
	C	7.3		
	H	25.2	21.8	
	F	14.2	24.6	6.9
Enrichment Ratio	Atoms	C	H	F
	C	**2.73**		
	H	0.17	**1.06**	
	F	0.70	**1.74**	0.00

NDFA: DFA				
Contact%	Atoms	C	H	F
	C	11.4	10.6	5.8
	F	7.2	39.1	26
Surface%		23.2	25.3	52.1
Random Contacts%	Atoms	C	H	F
	C	5.4		
	H	11.7	6.4	
	F	24.2	26.3	27.1
Enrichment Ratio	Atoms	C	H	F
	C	**2.12**		
	H	0.90	0.00	
	F	0.54	**1.49**	**1.92**
ADFA: DFA				
Contact%	Atoms	C	H	F
	C	18.1	7.1	2.1
	F	6.9	44.7	21
Surface%		26.15	25.9	47.9
Random Contacts%	Atoms	C	H	F
	C	6.8		
	H	13.5	6.7	
	F	25.0	24.8	22.9
Enrichment Ratio	Atoms	C	H	F
	C	**2.65**		
	H	0.52	0.00	
	F	0.36	**1.80**	**2.09**
TetDFA: DFA				
Contact%	Atoms	C	H	F
	C	21.2	5.2	0.6
	F	10.1	48.6	14.3
Surface%		29.15	26.9	44.0
Random Contacts%	Atoms	C	H	F
	C	8.5		
	H	15.7	7.2	
	F	25.6	23.6	19.3
Enrichment Ratio	Atoms	C	H	F
	C	**2.49**		
	H	0.33	0.00	
	F	0.42	**2.06**	**2.28**

Table S11. Enrichment ratios for the pairs of chemical species of the individual arene and decafluoroanthracene molecules of compounds **PyrDFA**, **PerDFA** and **TriDFA** at 100 K.

PyrDFA: Pyr				
Contact%	Atoms	C	H	F
	C	23.0	0.7	7.9
	H	3.8	25.6	39
Surface%		29.2	47.4	23.5
Random Contacts%	Atoms	C	H	F
	C	8.5		
	H	27.7	22.4	
	F	13.7	22.2	5.5
Enrichment Ratio	Atoms	C	H	F
	C	**2.70**		
	H	0.16	**1.14**	
	F	0.58	**1.76**	0.00

PyrDFA: DFA				
Contact%	Atoms	C	H	F
	C	20.8	4.7	1.7
	F	7.2	37.7	28
Surface%		27.6	21.2	51.3
Random Contacts%	Atoms	C	H	F
	C	7.6		
	H	11.7	4.5	
	F	28.3	21.8	26.3
Enrichment Ratio	Atoms	C	H	F
	C	**2.73**		
	H	0.40	0.00	
	F	0.31	**1.73**	**1.95**

PerDFA: Per				
Contact%	Atoms	C	H	F
	C	21.7	0.4	11.3
	H	2	22.2	42.4
Surface%		28.55	44.6	26.9
Random Contacts%	Atoms	C	H	F
	C	8.2		
	H	25.5	19.9	
	F	15.3	24.0	7.2
Enrichment Ratio	Atoms	C	H	F
	C	**2.66**		
	H	0.09	**1.12**	
	F	0.74	**1.77**	0.00

PerDFA: DFA				
Contact%	Atoms	C	H	F
	C	23.4	2.7	0.7
	F	12.2	48.3	12.6
Surface%		31.2	25.5	43.2
Random Contacts%	Atoms	C	H	F
	C	9.7		
	H	15.9	6.5	
	F	27.0	22.0	18.7
Enrichment Ratio	Atoms	C	H	F
	C	**2.40**		
	H	0.17	0.00	
	F	0.48	**2.19**	**2.31**

TriDFA: Tri				
Contact%	Atoms	C	H	F
	C	18.7	3.9	9.3
	H	7.5	19.9	40.9
Surface%		29.05	46.1	25.1
Random Contacts%	Atoms	C	H	F
	C	8.4		
	H	26.8	21.2	
	F	14.6	23.1	6.3
Enrichment Ratio	Atoms	C	H	F
	C	**2.22**		
	H	0.43	0.94	
	F	0.64	**1.77**	0.00

TriDFA: DFA				
Contact%	Atoms	C	H	F
	C	18.8	6.6	1.4
	F	8.6	46.1	18.6
Surface%		27.1	26.4	46.7
Random Contacts%	Atoms	C	H	F
	C	7.3		
	H	14.3	6.9	
	F	25.3	24.6	21.8
Enrichment Ratio	Atoms	C	H	F
	C	**2.56**		
	H	0.46	0.00	
	F	0.40	**1.88**	**2.14**

References

1. G. M. Sheldrick, SHELXT - Integrated space-group and crystal-structure determination, *Acta Crystallogr. Sect. A: Found. Crystallogr.*, 2015, **71**, 3-8.
2. G. M. Sheldrick, Crystal structure refinement with SHELXL, *Acta Crystallogr. Sec. C: Struct. Chem.*, 2015, **71**, 3-8.
3. C. B. Hübschle, G. M. Sheldrick and B. Dittrich, ShelXle: a Qt graphical user interface for SHELXL, *J. Appl. Crystallogr.*, 2011, **44**, 1281-1284.
4. H. Putz and K. Brandenburg, Diamond, Crystal and Molecular Structure Visualization, version 4.6.7, 2022,
5. O. V. Dolomanov, L. J. Bourhis, R. J. Gildea, J. A. K. Howard and H. Puschmann, OLEX2: a complete structure solution, refinement and analysis program, *J. Appl. Crystallogr.*, 2009, **42**, 339-341.
6. J. J. McKinnon, A. S. Mitchell and M. A. Spackman, Hirshfeld Surfaces: A New Tool for Visualising and Exploring Molecular Crystals, *Chem. Eur. J.* , 1998, **4**, 2136-2141.
7. J. J. McKinnon, M. A. Spackman and A. S. Mitchell, Novel tools for visualizing and exploring intermolecular interactions in molecular crystals, *Acta Crystallogr. B*, 2004, **60**, 627-668.
8. M. A. Spackman and D. Jayatilaka, Hirshfeld Surface Analysis, *CrystEngComm*, 2009, **11**, 19-32.
9. M. A. Spackman and P. G. Byrom, A novel definition of a molecule in a crystal, *Chem. Phys. Lett.*, 1997, **267**, 215-220.
10. P. R. Spackman, M. J. Turner, J. J. McKinnon, S. K. Wolff, D. J. Grimwood, D. Jayatilaka and M. A. Spackman, CrystalExplorer: a program for Hirshfeld surface analysis, visualization and quantitative analysis of molecular crystals, *J. Appl. Crystallogr.*, 2021, **54**, 1006-1011.
11. M. J. Turner, J. J. McKinnon, D. Jayatilaka and M. A. Spackman, Visualisation and characterisation of voids in crystalline materials, *CrystEngComm*, 2011, **13**, 1804-1813.
12. J. J. McKinnon, D. Jayatilaka and M. A. Spackman, Towards quantitative analysis of intermolecular interactions with Hirshfeld surfaces, *Chem. Commun.*, 2007, 3814–3816.
13. A. Parkin, G. Barr, W. Dong, C. J. Gilmore, D. Jayatilaka, J. J. McKinnon, M. A. Spackman and C. C. Wilson, Comparing entire crystal structures: structural genetic fingerprinting, *CrystEngComm*, 2007, **9**, 648-652.
14. M. A. Spackman and J. J. McKinnon, Fingerprinting intermolecular interactions in molecular crystals, *CrystEngComm*, 2002, **4**, 378-392.

15. J. P. Perdew, K. Burke and M. Ernzerhof, Generalized gradient approximation made simple, *Phys. Rev. Lett.*, 1996, **77**, 3865-3868.
16. S. J. Clark, M. D. Segall, C. J. Pickard, P. J. Hasnip, M. J. Probert, K. Refson and M. C. Payne, First principles methods using CASTEP, *Z. Kristallogr.*, 2005, **220**, 567-570.
17. J. F. Tannaci, M. Noji, J. McBee and T. D. Tilley, 9,10-dichlorooctafluoroanthracene as a building block for n-type organic semiconductors, *J. Org. Chem.*, 2007, **72**, 5567-5573.
18. G. Angulo, G. Grampp and A. Rosspeintner, Recalling the appropriate representation of electronic spectra, *Spectrochim. Acta Part A*, 2006, **65**, 727-731.
19. J. Mooney and P. Kambhampati, Get the Basics Right: Jacobian Conversion of Wavelength and Energy Scales for Quantitative Analysis of Emission Spectra, *J. Phys. Chem. Lett.*, 2013, **4**, 3316-3318.
20. D. Bischof, M. Zeplichal, S. Anhauser, A. Kumar, M. Kind, F. Kramer, M. Bolte, S. I. Ivlev, A. Terfort and G. Witte, Perfluorinated Acenes: Crystalline Phases, Polymorph-Selective Growth, and Optoelectronic Properties, *J. Phys. Chem. C*, 2021, **125**, 19000-19012.